A STUDY OF FLOW THROUGH VERY SHORT, SMALL CYLINDRICAL TUBES

Thesis for the Degree of M. S.

MICHIGAN STATE UNIVERSITY

Lowell C. Smith

1959

A STUDY OF FLOW
THROUGH VERY SHORT, SMALL CYLINDRICAL TUBES

By

LOWELL C. SMITH

AN ABSTRACT

Submitted to the College of Engineering
Michigan State University of Agriculture and Applied Science
in partial fulfillment of the requirements for the degree of

MASTER OF SCIENCE

Department of Mechanical Engineering

1959

Flow through very short cylindrical tubes differs from flow through long pipes in that the entrance and exit phenomena are the significant flow conditions. Both a theoretical and an experimental approach were employed in an attempt to predict the flow characteristics through the tube.

The theoretical approach requires a mathematical description of each flow zone within the tube. Then, to predict the flow characteristics of the entire tube, these mathematical descriptions must be linked together. Due to momentum considerations, the streamline bounding the main stream, or core flow, separates from the tube wall at the square edged entrance of the cylindrical tube. This separation continues to increase for a short distance downstream from the entrance. This is called the contraction zone. Downstream of the contraction zone, the streamlines diverge and approach the tube wall - the expansion zone. Normal pipe flow velocity profiles and friction considerations are considered to apply from this point downstream to the exit. Hence, a mathematical representation of flow through a very short, small cylindrical tube requires the joining of mathematical descriptions of four flow zones:

1. Contraction zone
2. Expansion zone
3. Pipe flow zone
4. Exit zone

Mathematical solutions are presently available for the pipe flow and exit zones. A numerical approximation to the streamline pattern in the contraction zone is also available. However, mathematical solutions to the equations describing the contraction and expansion zones will require a better understanding of the boundary layer and a mathematical representation of the flow boundary streamlines in these zones. Further investigation is required in these areas.

An experimental approach to flow through very short, small cylindrical tubes approximates this flow condition by a long orifice. Experimental determination of the orifice coefficient of discharge indicates the coefficient is markedly affected by the velocity of flow and the geometric characteristics of the cylindrical tube: length, diameter, and surface finish. Tests were conducted to determine the relationship between the geometric characteristics of the tube, the fluid properties, the fluid velocity, and the coefficient of discharge. The data obtained was plotted nondimensionally, and is considered to be generally applicable to any fluid flowing through any diameter tube subject only to the requirement of geometric similarity, i.e., equal L/D and e/D ratios for cylindrical tubes with a square edged entrance and exit configuration.

A STUDY OF FLOW
THROUGH VERY SHORT, SMALL CYLINDRICAL TUBES

By

LOWELL C. SMITH

A THESIS

Submitted to the College of Engineering
Michigan State University of Agriculture and Applied Science
in partial fulfillment of the requirements for the degree of

MASTER OF SCIENCE

Department of Mechanical Engineering

1959

TABLE OF CONTENTS

PRELIMINARIES

Page No.

SECTION I - THEORETICAL APPROACH

SECTION II - EXPERIMENTAL APPROACH

REFERENCE MATERIAL

LIST OF SYMBOLS

Symbol	Description	Units
A	cross-sectional area of cylindrical tube	in^2
A_s	cross-sectional area of the fluid	in^2
A_1	cross-sectional area at station 1	in^2
C	discharge coefficient	
C_c	contraction coefficient	
C_v	velocity coefficient	
d	diameter of flow boundary	in
D	diameter of cylindrical tube	in
e	surface roughness	microinches rms
F_p	pressure force	lb
F_s	shear force	lb
g	acceleration of gravity	in/sec^2
k	a constant	dimensionless
L	length of cylindrical tube	in
m	mass	$lb\text{-}sec^2/in$
M	momentum rate	lb
M_{BL}	momentum rate in the boundary layer	lb
M_c	momentum rate in the core	lb
P_e	pressure downstream from the tube exit	lb/in^2
P_s	pressure upstream from the tube entrance	lb/in^2
q	total velocity: $\vec{q} = \vec{u} + \vec{v}$	in/sec
Q	flow rate	in^3/sec or gpm
Q_{BL}	flow rate in boundary layer	in^3/sec
Q_c	flow rate in the core	in^3/sec
r	coordinate-radial distance outward from axis	in

Symbol	Description	Units
R	radius of cylindrical tube	in
t	time	sec
T	temperature	^{o}F
u	velocity component in x direction	in/sec
U	core velocity component in x direction	in/sec
v	velocity component in r direction	in/sec
V	average velocity in x direction	in/sec
x	axial distance	in
y	radial distance inward from tube wall	in
Z	elevation with respect to datum	in

GREEK SYMBOLS

α	asymptotic radius of contraction jet	in
β	temperature coefficient of viscosity	$1/^{o}F$
γ	weight density of fluid	lb/in^3
δ	boundary layer thickness	in
λ	temperature coefficient of density	$1/^{o}F$
μ	viscosity of fluid	$lb\text{-}sec/in^2$
ν	kinematic viscosity	in^2/sec
ξ	function of r and x	dimensionless
ρ	mass density of fluid	$lb\text{-}sec^2/in^4$
τ	shear stress	lb/in^2
τ_a	average shear stress	lb/in^2
τ_o	local shear stress	lb/in^2
φ	stream function	in^2

LIST OF FIGURES

FLOW THROUGH VERY SHORT, SMALL CYLINDRICAL TUBES

INTRODUCTION

Flow through very short cylindrical tubes differs from flow through long pipes in that the entrance and exit phenomena are the significant flow conditions. Actually, a very short pipe could be termed a long orifice.

The prediction of flow characteristic through very short, small cylindrical tubes may be approached in two ways. One approach is to mathematically describe each flow zone within the tube. Then, to predict the flow characteristics of the entire tube, these mathematical descriptions must be linked together. Verification of theory, by experiment, would be desirable.

Another approach is to consider the entire tube to be a long orifice, described by the flow equation:

$$Q = CA\sqrt{\frac{2\Delta P}{\rho}}$$

The value of the coefficient of discharge, C, may be determined experimentally.

CONCLUSIONS

Theoretical Analysis

An exact mathematical description of flow through a very short, small cylindrical tube is not now possible. A good mathematical approximation of the flow phenomena will require a better understanding of the boundary layer downstream of the inlet and a mathematical representation of the flow boundary streamlines in this region. Further work in these areas must precede solution of the equation describing this region.

Experimental Determination

Experimental determination of the orifice coefficient of discharge indicates the coefficient is markedly affected by the velocity of flow and the geometric characteristics of the cylindrical tube: length, diameter and surface finish. (See figure 1).

Cavitation occurred when the difference between the supply pressure and exhaust pressure, $P_s - P_e$, was very large. When cavitation was occurring, variation of P_e did not affect P_s. P_s was approximately constant during cavitating flow until P_e was increased to a critical pressure at which the cavitation ceased. The pressure difference, $P_s - P_e$, was approximately constant when the flow was without cavitation. Thus, the orifice coefficient of discharge is a function of P_s and P_e at low back pressure, P_e, when $P_s - P_e$ is large and cavitation occurs. The coefficient is not a function of P_s or P_e when non-cavitating flow occurs.

Figure 1 also indicates the coefficient of discharge is a linear function of $\frac{\rho Q}{\mu D}$ for values of $\frac{\rho Q}{\mu D}$ greater than 9,000.

It is the contention of Zucrow (8)* that the data plotted in figure 1 will apply to any fluid flowing through any diameter tube subject only to the requirement of geometric similarity, i.e., equal L/D ratios for cylindrical tubes with a square edged entrance and exit configuration. Further experimentation would be required to verify that contention.

---

* Numbers in parentheses refer to the List of References.

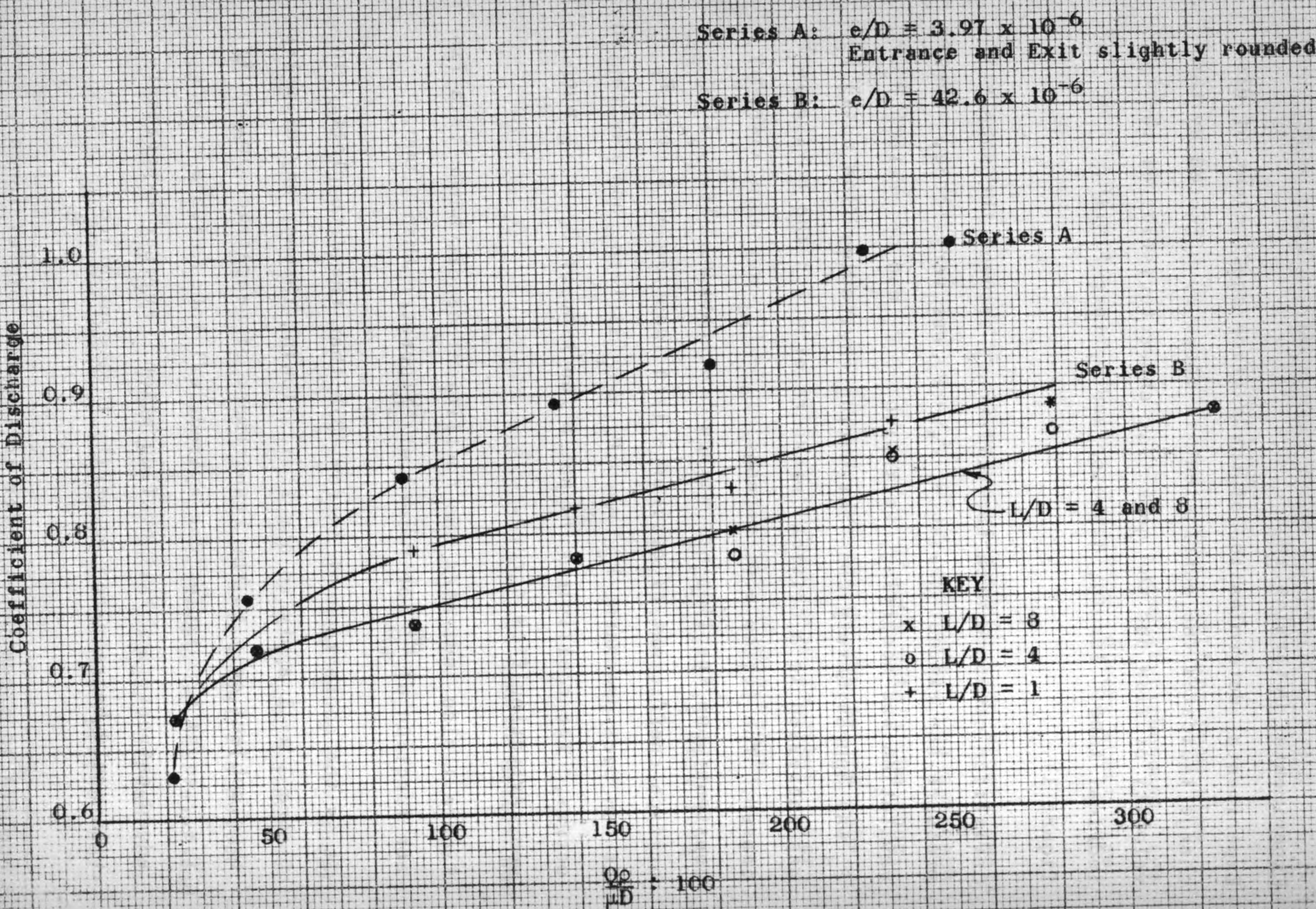

Plot of Experimental Points

Figure 1

SECTION I

THEORETICAL APPROACH

Scope of Theoretical Investigation

When fluid flows into a cylindrical tube through a square edged entrance, a contraction of the flow boundary occurs. The inflowing fluid particles have a radial velocity component as well as an axial velocity component. Particle inertia permits only a gradual turn at the square corner of the tube entrance, so the flow must separate from the tube wall. Between the wall of the tube and the streamline bounding the core flow area, a field of eddies is generated. Very little linear movement of these eddies occurs.

Downstream from the contraction, the flow boundary expands. A tube of sufficient length will allow enough expansion of the flow boundary to completely fill the tube. A portion of the problem is to determine the effect of various tube lengths upon pressure drop and quantity of flow through the tube. With long tubes, a normal boundary layer begins to develop at the point of reattachment.

The problem is to relate tube dimensions, fluid properties, and pressure difference to the quantity of flow. (See figure 2).

A mathematical representation of flow through a very short, small cylindrical tube requires the joining of mathematical descriptions of four separate flow zones:

1. Contraction zone near the tube entrance
2. Expansion zone
3. Pipe flow zone
4. Exit zone

Preliminary analysis was conducted assuming laminar flow. No attempt was made to represent theoretically, a turbulent or a cavitating flow condition.

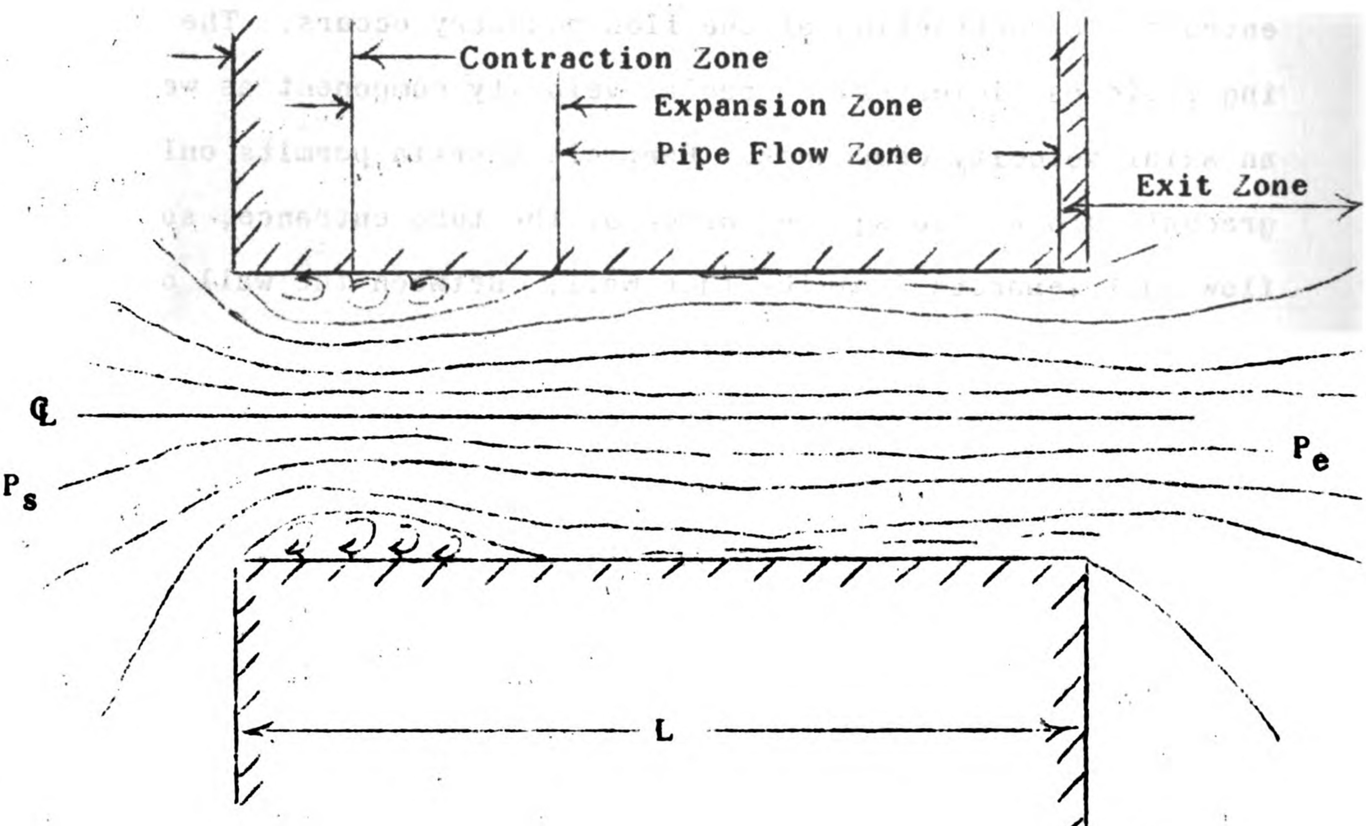

Flow Regions

$$Q = f\ (D,\ L/D,\ \mu,\ \rho,\ P_s - P_e,\ P_e,\ e)$$

Order of Magnitude

$$0.122 \leq D \leq 0.133$$

$$1 \leq L/D \leq 8.122$$

$$\mu_{150^oF} = 14.77 \times 10^{-7}\ \frac{\text{lb-sec}}{\text{in}^2}$$

$$\rho_{150^oF} = 8.37 \times 10^{-5}\ \frac{\text{lb-sec}^2}{\text{in}^4}$$

$$P_s \leq 3000 \text{ psi}$$

$$P_e \geq 40 \text{ psi}$$

Figure 2

Review of Previous Research

A survey of previous research produced treatments for three of the four flow regions discussed previously.

1. Contraction Zone

The contraction zone near the inlet may be likened to orifice flow in three dimensions with axial symmetry. This is very similar to the flow of fluid through an aperture of infinite length--a two dimensional problem. An exact soltion to this problem was arrived at by Kirchkoff in 1896 (1). Many authors have since repeated Kirchkoff's conformal transformations in the complex plane including a recent book in English by Strieter (2). Unfortunately, no exact solution to the similar three dimensional orifice has yet proven feasible (3). In 1913 Trefftz (4) determined, by successive approximation, that the coefficient of contraction for the three dimensional case of a circular orifice in an infinite plane boundary was between 0.60 and 0.62 as compared to a coefficient of 0.611 for the two dimensional case.

A description of the three dimensional jet profile with axial symmetry was accomplished by relaxation and published by Southwell and Vaisey (5). They consider an orifice plate in a circular tube. They compute a boundary error η defined by

$$\eta = \frac{1}{r} \frac{\partial \varphi}{\partial v} - k \qquad (1)$$

and reduce this error to zero (sensibly) along the streamline by modifying the streamline shape and the constant k.

Far downstream, the asymptotic solution was assumed to hold.

$$\varphi = \frac{1}{2} k r^2 \tag{2}$$

Let φ_B = the jet boundary streamline constant

α^2 = coefficient of contraction

Then $2\pi\varphi_B$ is the total flow through the orifice

α is the asymptotic radius when the orifice radius is unity.

From equation 2:

$$k\alpha^2 = 2\varphi_B \tag{3}$$

By assigning a value to φ_B, k may be accurately estimated, since α^2 is approximately known from hydraulic experiments. The solution, by relaxation to negligible error at all points is:

$$k = 118.34$$

$$\alpha^2 = (0.78)^2 = 0.6084$$

See figures 3, 4 and 5 from (5).

2. <u>Expansion Zone</u>

The expansion zone and reattachment of the flow boundary to the tube wall has not been previously described in mathematical detail.

3. <u>Pipe Flow Zone</u>

Brenkert (6) presents a calculational procedure for laminar flow and development of the boundary layer in a circular tube. Two assumptions are made:

a. Bernoulli equation (neglecting friction) can be applied to central core.

b. Velocity is constant across central core.

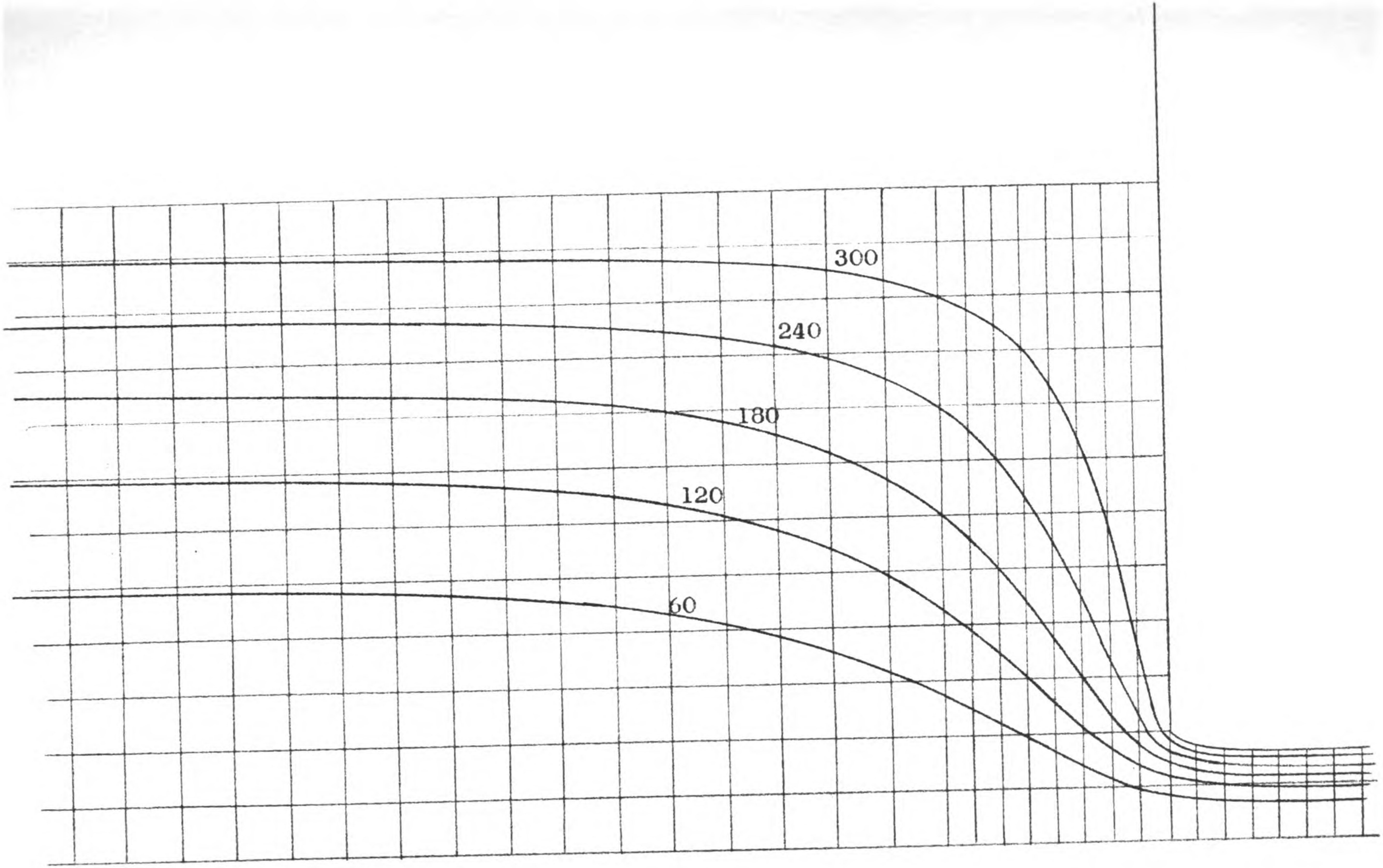

Plot of Streamlines near Orifice

Figure 3

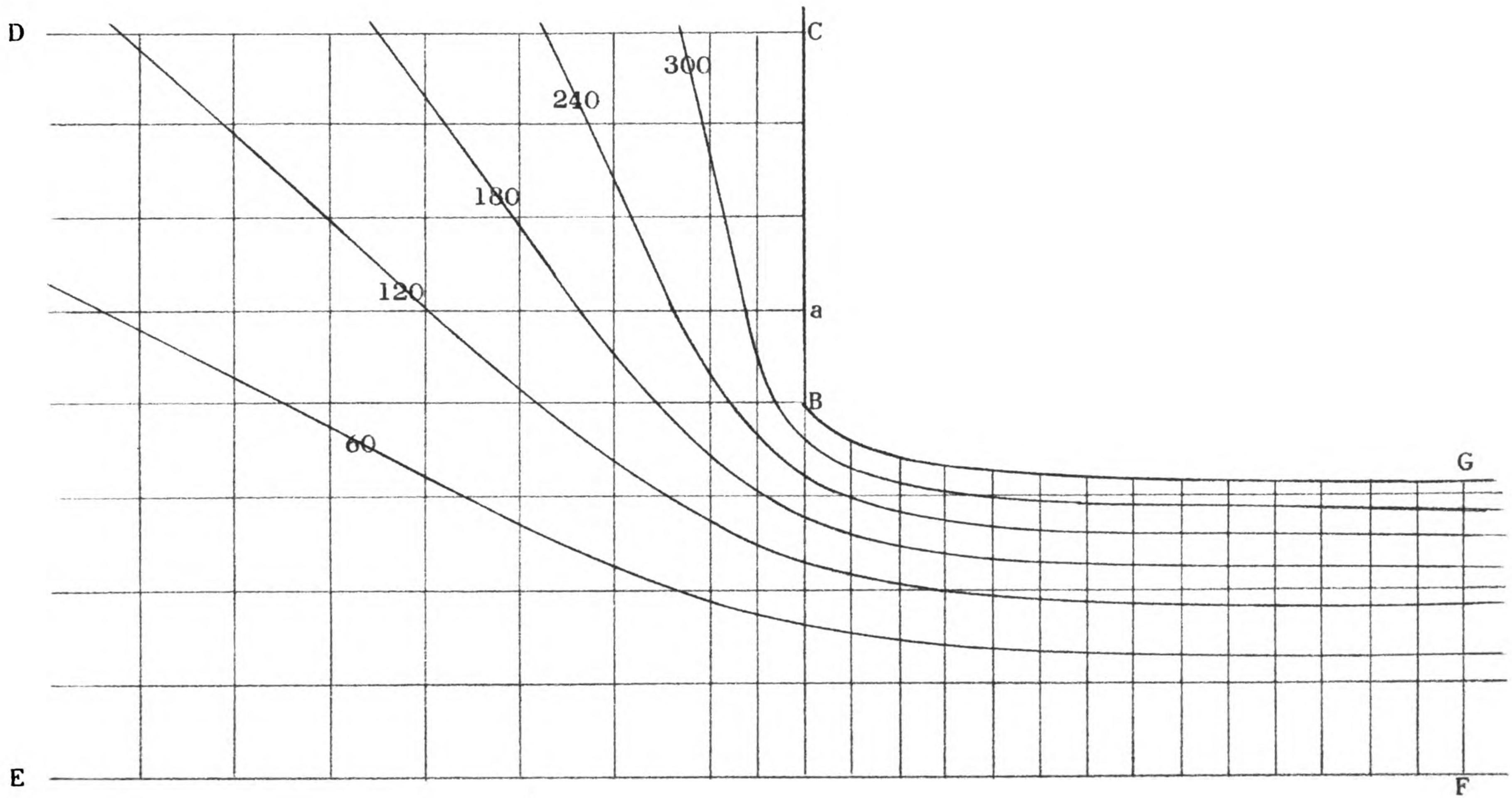

Plot of Streamlines near Orifice

Figure 4

Consider a control volume, figure 6:

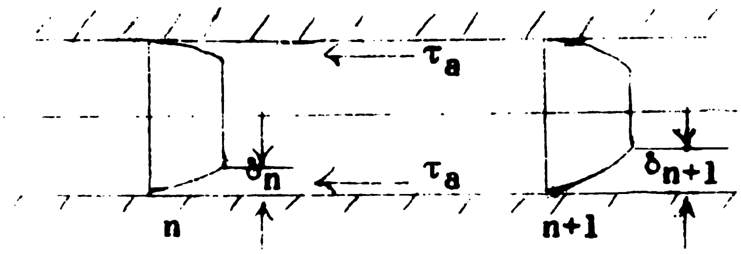

Control Volume

Figure 6

Apply Newton's Second Law:

$$\Sigma F_x = \frac{d}{dt}(mv)$$

$$P_n A - P_{n+1} A - 2\pi R x \tau_a = M_{n+1} - M_n$$

Solve for x:

$$x = \frac{(P_n - P_{n+1})A + M_n - M_{n+1}}{2\pi R \tau_a} \tag{4}$$

Evaluation of each of the terms in equation 4 follows:

$$M = M_{BL} + M_c \tag{5}$$

$$M_{BL} = \rho \int_{R-\delta}^{R} u^2 \, 2\pi r dr = 2\pi\rho \int_0^{\delta} u^2 \, (R-y) \, dy \tag{6}$$

$$M_c = \rho\pi \, (R-\delta)^2 \, U^2 \tag{7}$$

Substitute equations 6 and 7 into 5:

$$M = 2\pi\rho \int_0^{\delta} u^2 \, (R-y)dy + \rho\pi \, (R-\delta)^2 \, U^2 \tag{8}$$

The velocity is assumed constant across any core cross-section, i.e., viscous effects are considered appreciable only in the boundary layer. The modified cubic profile used by Shapiro, Siegel and Kline (4) most accurately describes the boundary layer velocity profile.

$$\frac{u}{U} = \left[\frac{3}{2}\left(\frac{y}{\delta}\right) - \frac{1}{2}\left(\frac{y}{\delta}\right)^3\right]\left[1 - \frac{\delta}{R}\right] + \left[2\left(\frac{y}{\delta}\right) - \left(\frac{y}{\delta}\right)^2\right]\left[\frac{\delta}{R}\right] \tag{9}$$

As $\frac{\delta}{R}$ increases from zero to unity, the cubic velocity profile changes to the parabolic form characteristic of fully developed flow through a circular pipe.

Rearrange equation 9 and let $k = \frac{\delta}{R}$

$$u = U\left[\frac{3}{2}\left(\frac{y}{\delta}\right) - \frac{1}{2}\left(\frac{y}{\delta}\right)^3 + \frac{1}{2}\,k\left(\frac{y}{\delta}\right) - k\left(\frac{y}{\delta}\right)^2 + \frac{1}{2}\,k\left(\frac{y}{\delta}\right)^3\right] \tag{10}$$

Substitute equation 10 into equation 8, integrate and simplify:

$$M = \rho A V^2\left[1 - \frac{36}{35}\,k + \frac{677}{1680}\,k^2 + \frac{107}{840}\,k^3 - \frac{1}{560}\,k^4\right] \tag{11}$$

Thus, for each assumed boundary layer thickness, the momentum rate may be calculated.

Pressure is assumed constant over the cross-section. In the central core apply Bernoulli's equation:

$$\frac{P}{\gamma} + \frac{U^2}{2g} = \text{constant} \tag{12}$$

In order to calculate pressure, the velocity must be first calculated.

To satisfy continuity, the flow rate Q must be a constant at every cross-section of the pipe.

$$Q = Q_{BL} + Q_c \tag{13}$$

Consider the cross-section of a uniform pipe shown in figure 7.

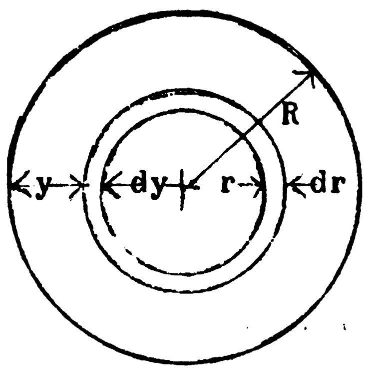

Cross-section of a Uniform Pipe

Figure 7

$$Q_{BL} = \int_{R-\delta}^{R} u\ 2\pi r dr = 2\pi \int_{0}^{\delta} u\ (R-y) dy \tag{14}$$

$$Q_c = \pi\ (R-\delta)^2\ U \tag{15}$$

Substitute equations 14 and 15 into 13:

$$Q = 2\pi \int_0^\delta u(R-y)dy + \pi(R-\delta)^2\ U \tag{16}$$

Substitute equation 9 into 16 and let $Q = VA$

$$VA = 2\pi U \int_0^\delta \left[\frac{3}{2}\left(\frac{y}{\delta}\right) - \frac{1}{2}\left(\frac{y}{\delta}\right)^3 + \frac{1}{2}\ k\left(\frac{y}{\delta}\right) - k\left(\frac{y}{\delta}\right)^2 + \frac{1}{2}\ k\left(\frac{y}{\delta}\right)^3\right](R-y)dy + \pi(R-\delta)^2 U$$

Integrate and simplify:

$$\frac{V}{U} = \frac{60 - 45\ k + 17\ k^2 - 2k^3}{60} \tag{17}$$

Consider the definition of shear stress:

$$\tau_o = \mu\ \frac{du}{dy} \tag{18}$$

Substitute equation 9 into 18:

$$\tau_o = \mu U\ \frac{d}{dy}\left[\frac{3}{2}\left(\frac{y}{\delta}\right) - \frac{1}{2}\left(\frac{y}{\delta}\right)^3 + \frac{1}{2}\ k\left(\frac{y}{\delta}\right) - k\left(\frac{y}{\delta}\right)^2 + \frac{k}{2}\left(\frac{y}{\delta}\right)^3\right]$$

Differentiate and let $y \rightarrow 0$ to get wall shear stress

$$\tau_o = \mu U \left[\frac{3}{28} + \frac{k}{28}\right]$$

$$\tau_o = \frac{\mu U}{28}\left[3 + k\right] \tag{19}$$

For the average shear stress between station n and station n+1, compute:

$$\tau_a = \frac{\tau_{o_n} + \tau_{o_{n+1}}}{2} \tag{20}$$

Special assumptions must be made at the beginning of the pipe flow boundary layer development. Equation 19 indicates an infinite shear stress for $\delta = 0$. Thus, the boundary layer thickness at the inlet of the pipe flow zone must be assumed equal to some finite value. This infers that the streamline bounding the core flow does not reattach itself to the tube wall, but only approaches the wall. A boundary layer of finite thickness separates the tube wall and the streamline bounding core flow.

The flow in the tube downstream from the reattachment, can be completely described by use of known fluid properties and the proceeding equations 4, 11, 12, 17, 19 and 20.

4. Exit Zone

Schlicting (7) presents an analytical treatment of a jet formed by fluid flowing out of a small circular opening and mixing with similar surrounding fluid.

The pressure along the axis of the jet is assumed constant. From this assumption, efflux of momentum in x direction is given by:

$$M = 2\pi\rho \int_0^\infty u^2 \, r dr = \text{constant} \qquad (21)$$

Equation of motion in x direction

$$u \frac{\partial u}{\partial x} + v \frac{\partial u}{\partial r} = \nu \frac{1}{r} \frac{\partial}{\partial r} \left(r \frac{\partial u}{\partial r} \right) \qquad (22)$$

Continuity equation

$$\frac{\partial u}{\partial x} + \frac{\partial v}{\partial r} + \frac{v}{r} = 0 \qquad (23)$$

Boundary conditions

a. u is maximum on jet axis

$$r = 0: \quad v = 0 \quad \frac{\partial u}{\partial r} = 0$$

b. fluid at infinity is at rest

$$r = \infty: \quad u = 0$$

c. velocity profiles; u(x,r) are assumed similar

From equation 21 the momentum is seen not to be a function of x. Equation 22 indicates that the inertia and frictional terms are of the same order of magnitude. The solution may be obtained in the form:

$$\varphi = \nu x g(\eta) \qquad \text{where } \eta = \frac{1}{\nu^{1/2}} \frac{r}{x} \tag{24}$$

The equation of continuity must be satisfied. Therefore the stream function φ must satisfy:

$$u = \frac{1}{r}\frac{\partial \varphi}{\partial r} \qquad \text{and} \qquad v = -\frac{1}{r}\frac{\partial \varphi}{\partial x}$$

This makes:

$$u = \frac{1}{r}\frac{\partial}{\partial r} \quad \nu x g(\eta) \quad = \frac{g'}{\eta x}$$

$$v = -\frac{1}{r}\frac{\partial}{\partial x}\left[\nu x g(\eta)\right] = \frac{\nu^{1/2}}{x}\left(g' - \frac{g}{\eta}\right) \tag{25}$$

The equation for g is:

$$-\frac{d}{d\eta}\left(\frac{gg'}{\eta}\right) = \frac{d}{d\eta}\left(g'' - \frac{g'}{\eta}\right) \tag{26}$$

In terms of g, the boundary conditions become:

$$g'(\infty) = 0$$

$$\eta = 0 \qquad g(0) = g'(0) = 0$$

Since $\frac{gg'}{\eta}$ and $g'' - \frac{g'}{\eta}$ both vanish at the origin, equation 26 may be integrated in the form:

$$\eta g'' - g' + gg' = 0 \tag{27}$$

The particular solution of equation 27 is:

$$g = \frac{\xi^2}{1 + \frac{1}{4}\xi^2} \quad \text{where } \xi = k\eta \tag{28}$$

This makes:

$$u = \frac{2k^2}{x\left(1 + \frac{1}{4}\xi^2\right)^2}$$

and then:

$$M = \frac{16}{3}\pi\mu k^2 \tag{29}$$

Hence:

$$u = \frac{3M}{8\pi\mu x}\,\frac{1}{\left(1 + \frac{1}{4}\xi^2\right)^2}$$

$$v = \frac{1}{4}\left(\frac{3M}{\pi\rho}\right)^{1/2}\frac{1}{x}\,\frac{\xi\left(1 - \frac{1}{4}\xi^2\right)}{\left(1 + \frac{1}{4}\xi^2\right)^2} \tag{30}$$

where: $\xi = \frac{1}{4\nu}\left(\frac{3M}{\pi\rho}\right)^{1/2}\frac{r}{x}$

The flow volume is easily computed:

$$Q = 2\pi\int_0^\infty u r\,dr = 8\pi\nu x \tag{31}$$

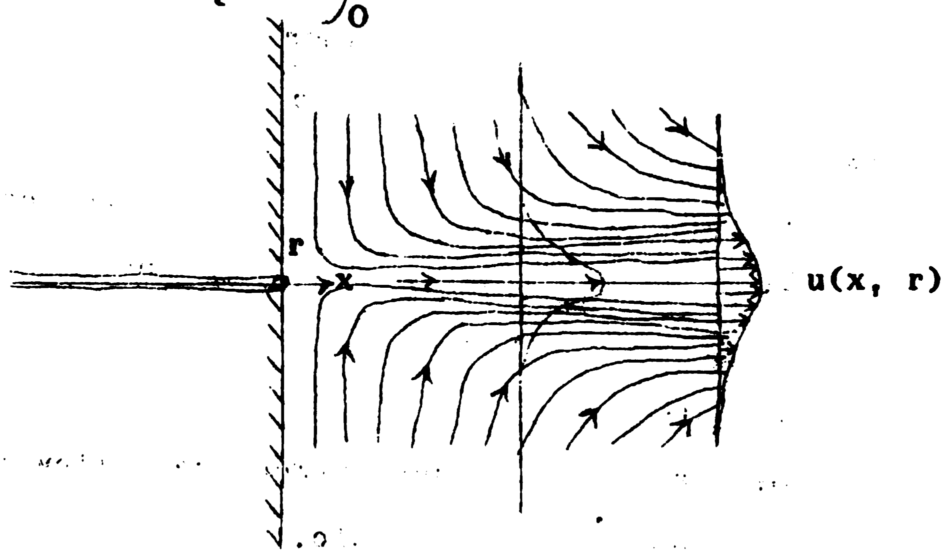

Streamline Pattern for a Circular Laminar Jet

Figure 8

ANALYSIS

The first step in a complete mathematical description of a short cylindrical tube is to completely describe each flow zone and transitions, if any, in a compatible coordinate system. Adaptations of the work of Brenkert and Schlicting will describe the pipe flow zone and exit zone.* The contraction and expansion zones require further original development.

Consider the forces acting upon an element of volume within the contracting flow region.

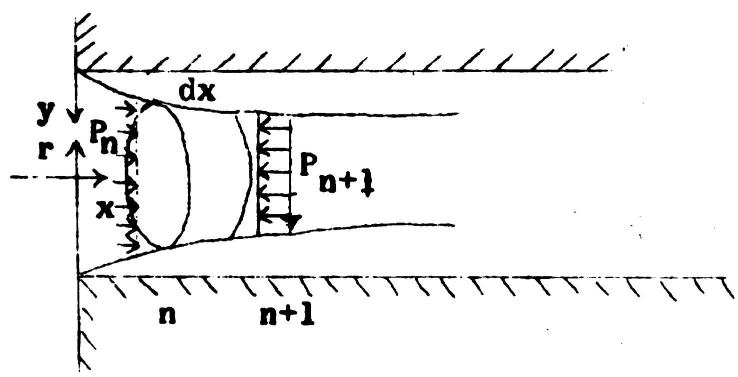

Volume Element

Figure 9

Assumptions

1. Pressure is constant across core section.
2. Flow is symmetrical with respect to axis.
3. Fluid is Newtonian.
4. Steady state.
5. Mass interchange between core flow and boundary eddies is negligible.

Apply Newton's Second Law

$$\Sigma F_x = \frac{d}{dt}(mu)$$

F_p, the pressure force, may be calculated from the following considerations:

$$\text{radius at station } n = r - \frac{\partial r}{\partial x}\frac{dx}{2}$$

$$\text{area at station } n = \pi\left(r - \frac{\partial r}{\partial x}\frac{dx}{2}\right)^2$$

Therefore:

$$F_{P_n} = \left(P - \frac{\partial P}{\partial x}\frac{dx}{2}\right)\pi\left(r - \frac{\partial r}{\partial x}\frac{dx}{2}\right)^2$$

Similarly:

$$F_{P_{n+1}} = \left(P + \frac{\partial P}{\partial x}\frac{dx}{2}\right)\pi\left(r + \frac{\partial r}{\partial x}\frac{dx}{2}\right)^2$$

F_s, the average shear force, is obtained by considering the definition of shear stress.

$$\tau = \mu\frac{du}{dr}$$

Therefore: $F_s = \tau A$ where $A = 2\pi r dx$

Substituting:

$$F_s = \mu\frac{du}{dr}2\pi r dx$$

Assume the shear stress at the midpoint between stations n and (n+1) is equal to the average shear stress between stations n and (n+1).

Momentum change, the right hand term in Newton's Second Law, is obtained from the following considerations.

From the definition of a total derivative:

$$\frac{d}{dt}(mu) = \frac{\partial}{\partial x}(mu)\frac{dx}{dt} + \frac{\partial}{\partial r}(mu)\frac{dr}{dt} + \frac{\partial}{\partial t}(mu)$$

From the assumptions of steady state and negligible mass interchange between core flow and the boundary layer.

$$\frac{d}{dt}\,(mu) = m\,\frac{\partial u}{\partial x}\,\frac{dx}{dt} + m\,\frac{\partial u}{\partial r}\,\frac{dr}{dt}$$

Since u >>> v, i.e., $\frac{dx}{dt} >>> \frac{dv}{dt}$, and q is considered constant across any core cross section, then $\frac{\partial u}{\partial r} \sim 0$ and the last term in the preceding equation may be neglected.

$$\frac{d}{dt}\,(mu) = m\,\frac{\partial u}{\partial x}\,u$$

$$\frac{d}{dt}\,(mu) = \rho\pi r^2 u\,\frac{\partial u}{\partial x}\,dx$$

where mass = density x volume = $\rho\pi r^2 dx$

Substitute the above quantities in Newton's Second Law:

$$\left(P - \frac{\partial P}{\partial x}\,\frac{dx}{2}\right)\pi\left(r - \frac{\partial r}{\partial x}\,\frac{dx}{2}\right)^2 - \left(P + \frac{\partial P}{\partial x}\,\frac{dx}{2}\right)\pi\left(r + \frac{\partial r}{\partial x}\,\frac{dx}{2}\right)^2$$
$$- 2\pi\mu r\,\frac{du}{dr}\,dx - \rho\pi r^2 u\,\frac{\partial u}{\partial x}\,dx = 0$$

Expand squared terms and multiply through by $\frac{1}{\pi}$

$$\left(P - \frac{\partial P}{\partial x}\,\frac{dx}{2}\right)\left[r^2 - r\,\frac{\partial r}{\partial x}\,dx + \left(\frac{\partial r}{\partial x}\,\frac{dx}{2}\right)^2\right] - \left(P + \frac{\partial P}{\partial x}\,\frac{dx}{2}\right)\left[r^2 + r\,\frac{\partial r}{\partial x}\,dx + \left(\frac{\partial r}{\partial x}\,dx\right)^2\right]$$
$$- 2\mu r\,\frac{du}{dr}\,dx - \rho r^2 u\,\frac{\partial u}{\partial x}\,dx = 0$$

Neglect $\left(\frac{\partial r}{\partial x}\,\frac{dx}{2}\right)^2$ in comparison with $\frac{\partial r}{\partial x}\,dx$, an infinitesimal of higher order in comparison with $\frac{\partial r}{\partial x}\,dx$.

Expand equation:

$$-r^2\,\frac{\partial P}{\partial x}\,dx - 2Pr\,\frac{\partial r}{\partial x}\,dx - 2\mu r\,\frac{du}{dr}\,dx - \rho r^2 u\,\frac{\partial u}{\partial x}\,dx = 0$$

Multiply through by $-\frac{1}{rdx}$:

$$r \frac{\partial P}{\partial x} + 2P \frac{\partial r}{\partial x} + 2\mu \frac{du}{dr} + \rho r u \frac{\partial u}{\partial x} = 0 \qquad (32)$$

Discussion of Physical Significance

$\frac{\partial P}{\partial x}$ is negative and mainly a function of the velocity increase through the contracting flow region and, to a negligible extent, a function of frictional losses. The second effect may be ignored in comparison with the magnitude of the first. Thus, $\frac{\partial P}{\partial x}$ is a function of the flow streamline boundary.

$\frac{\partial r}{\partial x}$ is negative and definitely a function of the flow streamline boundary.

$\frac{\partial u}{\partial r}$ is negative and refers to the sizeable change in axial velocity as r increases from just within the core section to just inside the eddy field bounding the core section.

$\frac{\partial u}{\partial x}$ is positive. This is the change in velocity required by continuity with a change in flow cross section--thus a function of the flow streamline boundary.

DISCUSSION

The difficulties encountered in solving the partial differential equation can readily be seen. To date, the streamline bounding core flow has not been described mathematically. The numerical solution is approximately correct at the relaxation nodes, but it is not continuous nor does it have derivatives. Thus, $\frac{\partial P}{\partial x}$, $\frac{\partial r}{\partial x}$ and $\frac{\partial u}{\partial x}$ cannot be obtained, since all depend directly or indirectly on the partial derivatives of the equation of the flow boundary. No method of deriving this equation is presently available.

Evaluation of $\frac{\partial u}{\partial r}$ is also very difficult, due to our present lack of understanding of the eddy field bounding the core flow and the interaction between the two flow regions.

An analysis of the expanding flow zone is very similar to the preceding development. The force equations are identical. However, when evaluated, the gradients will be opposite in sign. Just as in the contracting flow zone, the lack of a mathematical equation of the streamline boundary of core flow and an understanding of the eddy field bounding the core flow, prevent solution for the expanding flow zone.

SECTION II

EXPERIMENTAL APPROACH

Scope of Experimental Investigation

An experimental determination of the flow characteristics through short, small cylindrical tubes delves into variations of arbitrary coefficients which modify theoretical flow equations. The orifice flow equation is:

$$Q = CA\sqrt{\frac{2\Delta P}{\rho}}$$

The coefficient of discharge, C, modifies a theoretical description of frictionless flow through an infinitely thin orifice. This coefficient is affected by the properties of the fluid, finite thickness of orifice wall, surface roughness, and the inlet and exit configurations in practical applications. This experimental investigation is intended to:

1. Isolate unimportant factors.
2. Determine magnitude of each effect.

Review of Previous Research

Zucrow (8) investigated the flow of benzol through submerged tubes of small diameter ($0.020 \leq D \leq 0.088$). Among his important conclusions are:

1. If C, the coefficient of discharge, is plotted as a function of $W\Phi r$, the characteristic curve is valid for all jets which are geometrically similar. Where:

   W = actual rate of discharge

   Φ = fluidity of the liquid = $\frac{1}{\mu}$

   r = reciprocal of diameter = $\frac{1}{d}$

2. Square-edged jets are geometrically similar when they have equal values of L/D.

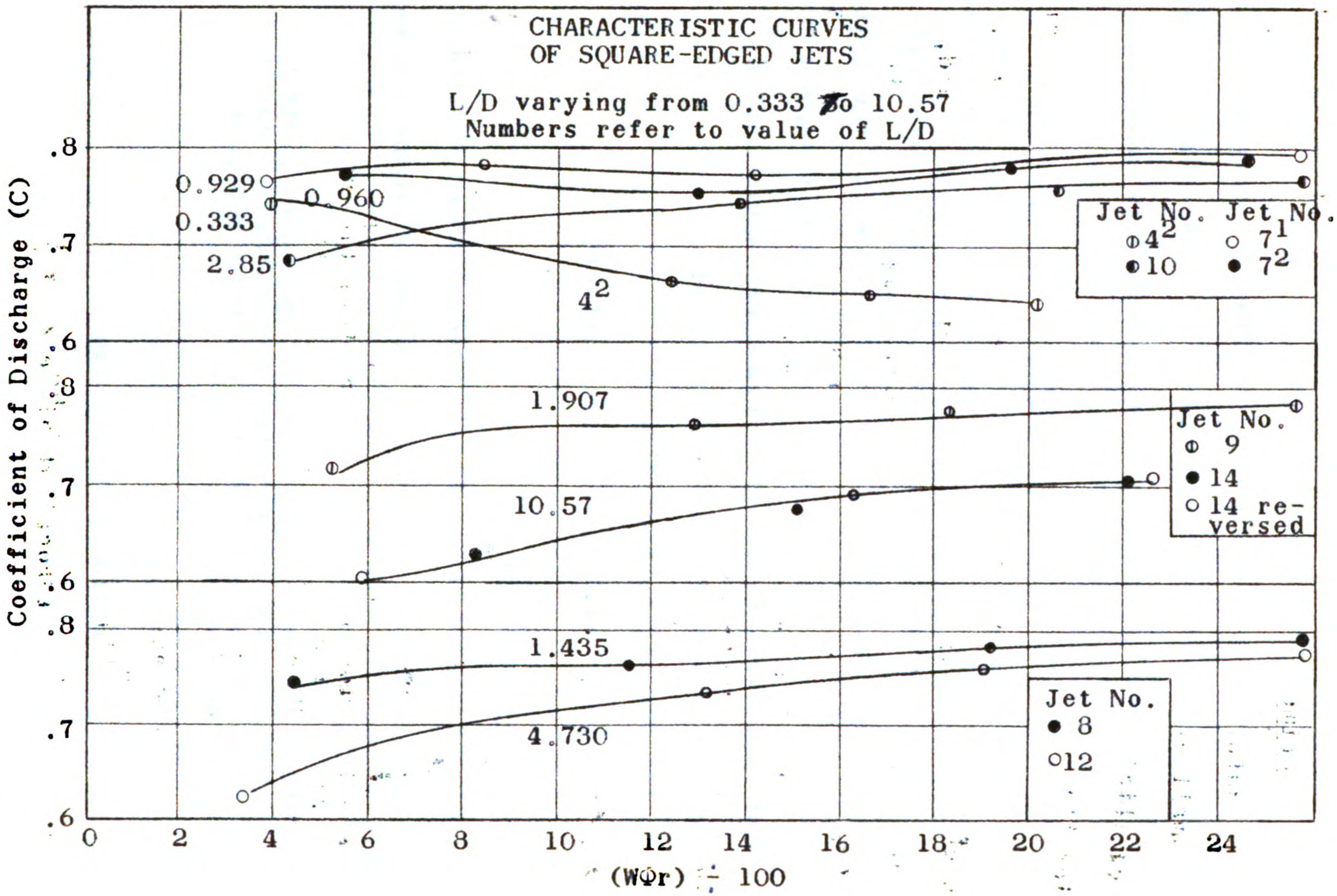

Characteristic Curves for Square-Edged Jets with Different Values of L/D

Figure 10

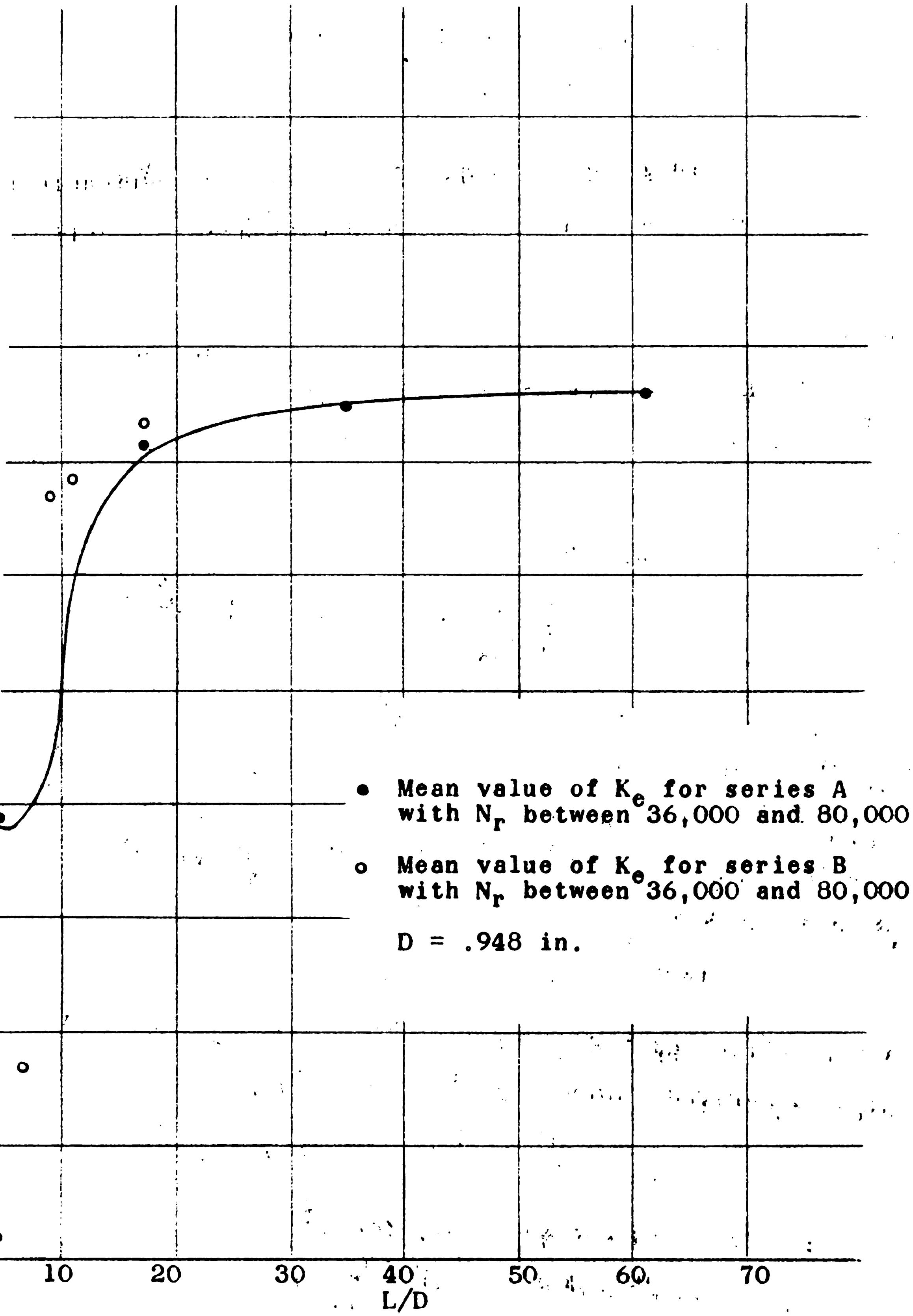

Coefficient of Entrance Loss of a Square-Edged Inlet

Figure 11

Figure 10 shows the characteristic curves for square-edged jets with L/D ratios of 0.333 to 10.57.

Portions of a thesis by Chia-Tsun Chen (9) are applicable to flow characteristics near the square-edged entrance of a cylindrical tube.

To investigate flow through the outlet pipe at the bottom of a tank, consider the following equation:

$$H = \frac{V^2}{2g} + f\,\frac{L}{D}\,\frac{V^2}{2g} + K_e\,\frac{V^2}{2g} \tag{33}$$

where: H = total head, ft

V = mean velocity over the section, in/sec

f = Darcy friction factor

K_e = coefficient of entrance loss

Direct experimental measurements of H and V and theoretical calculation of f enables K_e to be determined from equation 33. The plot of K_e versus L/D, figure 11, has a very significant minimum at an L/D ratio between 3 and 4.

ANALYSIS

A theoretical approximation to flow through a very, very short pipe is derived from Bernoulli's equation.

$$\frac{P_s}{\rho} + gZ_s + \frac{1}{2}\,q_s^2 = \frac{P_1}{\rho} + gZ_1 + \frac{1}{2}\,q_1^2$$

where: P_s = supply pressure, lb/in^2

P_1 = pressure at pipe exit, lb/in^2

Z_s = elevation of pipe inlet, in

Z_1 = elevation of pipe outlet, in

q_s = total velocity preceding pipe inlet, in/sec

q_1 = total velocity at pipe exit, in/sec

For every large area ratio, $A_s >>> A_1$, and thus $q_s <<< q_1$. Therefore $q_s \approx 0$. Also, since the pipe is very short, $Z_s \sim Z_1$, regardless of the orientation of the pipe.

Thus: $$\frac{P_s}{\rho} = \frac{P_1}{\rho} + \frac{1}{2} q_1^2$$

Rearranging: $$q_1 = \sqrt{\frac{2(P_s - P_1)}{\rho}} \qquad (35)$$

To find total flow through the small cylindrical tube, consider the continuity equation:

$$Q = q\ A \qquad (36)$$

Substitute equation 35 into 36:

$$Q = A\sqrt{\frac{2(P_s - P_1)}{\rho}} \qquad (37)$$

Equation 37 applies only to frictionless flow. For actual flow conditions, the equation must be modified to account for entrance losses, the reduction in effective tube cross sectional area due to flow contraction just downstream from the tube entrance, fluid friction along the tube, and exit losses. Thus, for actual flow:

$$Q = CA\sqrt{\frac{2(P_s - P_1)}{\rho}} \qquad (38)$$

where: $C = C_c C_v$

C_c, the contraction coefficient, is attributed to the inability of the radially moving fluid particles to instantaneously change direction of travel to an axial direction at the sharp-edged entry of the tube. Hence, the fluid flow area contracts near the tube entrance. For a very short tube, an orifice, $C_c = 0.6$, meaning that the flow area is only 60% of total orifice area. In longer tubes, an expansion follows the contraction but sizeable losses occur in the contraction-expansion process. C_c is a function of fluid momentum and the tube geometry.

C_v, the velocity coefficient, is attributed to frictional losses along the tube wall and fluid friction. Wall friction is a function of fluid properties, surface finish, and geometry. Fluid friction is a function of fluid properties and flow quantity.

Thus: $C = f(\rho, V, \mu, D, L, e)$

Since: $C = C_c C_v$

where: $C_c = f(\rho, V, L, D)$

$C_v = f(\rho, \mu, e, L, D, V)$

For actual experimental purposes, the quantity of flow, Q, may be measured directly. Velocity, V, is obtained by calculation from the equation $Q = VA$. It was decided to consider $C = f(Q)$ for the purpose of simplifying the recording of experimental data.

Therefore: $C = f(\rho, Q, \mu, D, L, e)$

Dimensional analysis

Dimensions: $\rho \quad \frac{\text{lb-sec}^2}{\text{in}^4} = FL^{-4}\,T^2$

$Q \quad \frac{\text{in}^3}{\text{sec}} = L^3\,T^{-1}$

$\mu \quad \frac{\text{lb-sec}}{\text{in}^2} = F\,L^{-2}\,T$

$D, L, e \text{ (in)} = L$

Dimensional Matrix:

	ρ	Q	μ	D	L	e
Force: F	1	0	1	0	0	0
Length: L	-4	3	-2	1	1	1
Time: T	2	-1	1	0	0	0

From F: $0 = \rho + \mu$ (39)

From L: $0 = -4\rho + 3Q - 2\mu + D + L + e$ (40)

From T: $0 = 2\rho - Q + \mu$ (41)

Solve equation 39 for μ: $\mu = -\rho$ (42)

Solve equation 41 for Q: $Q = 2\rho + \mu$

Substitute equation 42: $Q = 2\rho - \rho$

Collect like terms: $Q = \rho$ (43)

Solve equation 40 for D: $D = 4\rho - 3Q + 2\mu - L - e$

Substitue equations 42 and 43:

$$D = 4\rho - 3\rho - 2\rho - L - e$$

Collect like terms: $D = -\rho - L - e$ (44)

From equations 42, 43 and 44 construct the π matrix.

	ρ	Q	μ	D	L	e
π_1 (ρ)	1	1	-1	-1	0	0
π_2 (L)	0	0	0	-1	1	0
π_3 (e)	0	0	0	-1	0	1

Therefore: $\pi_1 = \frac{\rho Q}{\mu D}$

$$\pi_2 = \frac{L}{D}$$

$$\pi_3 = \frac{e}{D}$$

The coefficient of discharge can now be expressed in terms of nondimensional parameters thusly:

$$C_D = f\left(\frac{\rho Q}{\mu D},\ \frac{L}{D},\ \frac{e}{D}\right) \qquad (45)$$

Experimental Method

Recall the relationships:

$$Q = CA\sqrt{\frac{2(P_s - P_e)}{\rho}} \qquad (38)$$

and

$$C = f\left(\frac{\rho Q}{\mu D},\ \frac{L}{D},\ \frac{e}{D}\right) \qquad (45)$$

ρ and μ are determined by the fluid and fluid temperature. A, L, D and e are dimensions which may be measured directly or computed from simple basic formulas. Experimental values of Q and $P_s - P_e$ may be measured directly. The values of C may be computed from equation 38 and experimental data. By varying Q, L, D and e, the relationship suggested in equation 45 may be investigated.

Experimental Equipment

Small cylindrical tubes were made by drilling, reaming and, in some cases, polishing a small hole through a special test block (see Appendix D). The L/D ratio was varied between 8 and 1 by reducing the length of the hole. The sharp edge of the tube inlet and outlet was compared by microscopic inspection and protected from damage at all times. Steel and plastic test blocks were used. Holes in the steel test block were drilled and reamed yielding a microinch finish of between 50 and 55 rms. Holes in the plastic test block were drilled, step reamed and polished, resulting in a microinch finish between 4 and 6 rms--an optically clear surface, permitting visual observation of the flow phenomena. Finished hole sizes ranged from 0.122 inches to 0.133 inches.

The plans of the entire test fixture are included in Appendix D. A forty power microscope and microscope light were mounted in the microscope mount, which could be indexed along the length of the cylindrical tube. Careful, accurate observation of flow conditions was therefore possible.

Pressure taps were located 48 diameters upstream from the tube entrance and downstream from the tube exit to measure P_s and P_e respectively. Thermocouples, located at the same position, measured T_s and T_e. Two turbine type flow pickups located downstream from the pressure tap and thermocouple were employed. The capacity of the smaller one was from 0.3 to 2.2 gallons per minute; the capacity of the larger one from 2 to 24 gallons per minute. Valving permitted flow to be directed into either of the flow pickups. Thus, flows from 0.3 to 24 gallons per minute could be accurately measured.

The flow output of the variable delivery pump was manually controlled from negligible flow to 14 gallons per minute. The pump required a supply of oil at a pressure of 40 to 50 psi. This was accomplished by pressurizing the reservoir with compressed air acting on the fluid surface. Thus, the reservoir pressure, pump supply pressure, and reservoir return pressure was 45 ± 5 psig. All reservoir connections were submerged. Pump output pressure was determined by: resistance to flow in the system, pressure drop across the test block, and adjustable pressure drop across the needle valve. Line losses were considered negligible. The cross-sectional area of the lines was no less than 25 times the cross-sectional area of the cylindrical tube under investigation. The assumption of negligible line losses is therefore quite good. The pressure drop across a given test block is determined by the quantity of fluid flowing. A needle valve, downstream of the test block, was employed to vary the back pressure on the test block -- hence, the pressure range at which the pressure drop across the test block occurred.

Test Procedure

Warm up of the system was accomplished by an electric heater in the reservoir. Temperature was maintained by heating or cooling the fluid as required. The heater was controlled by a thermostat device whose sensing element was in the reservoir. Cooling was controlled manually by adjusting the quantity of cooling water flowing through the heat exchanger.

For each length and diameter of tube investigated, a series of runs was made. Runs were conducted at flow quantities of 1, 2, 4, 6, 8, 10, 12 and 14 gallons per minute. The test block exit pressure was varied from 50 psig to (3000 psig - ΔP) by adjusting the needle valve. After each adjustment in back pressure, the flow quantity and the temperature of the fluid were adjusted, if necessary, before the data were recorded.

Each test block was run and checked in the reversed direction of flow to detect any noticeable discrepancies due to edge sharpness or surface irregularities.

Discussion

A nondimensional plot of C versus $\frac{\rho Q}{\mu D}$ indicates the coefficient increases as the quantity of flow increases--a rather sharp initial rise and less steep linear rise for further increases in $\frac{\rho Q}{\mu D}$. The surface finish of the cylindrical tube appears to have a very important influence on the coefficient--certainly as important as the L/D ratio. See figure 1. It must also be noted that the cylindrical tube in the plastic test block was not truly cylindrical. When the tube walls were polished, the entrance and exit of the tube were enlarged slightly.

LIST OF REFERENCES

1. Kirchkoff, G., "Zur Theorie Freier Flüssigkeitsstrahlen", Crelles Journal, Vol. 70, 1869, p. 289.

2. Strieter, V. L., Fluid Dynamics, McGraw-Hill Book Co., Inc., 1948, pp. 174-177.

3. Rouse, H. and Abdel-Hadi Abul-Fetouh, "Characteristics of Irrotational Flow through Axially Symmetric Orifices", Journal of Applied Mechanics, Dec. 1950, pp. 421-426.

4. Trefftz, V. E., "Über die Kontraktion Kreisförmiger Flüssigkeitsstrahlen", Zeitschrift für Mathematik and Physik, Vol. 64, 1917, p. 34.

5. Southwell, R. V. and Vaisey, G., "Relaxation Methods Applied to Engineering Problems - Fluid Motions Characterized by Free Streamlines", Proc. Roy. Soc., Vol. 240 A, pp. 117-127 and pp. 134-141.

6. Brenkert, K., "A Study of Pressure Variation in the Region of Boundary Layer Transition in Cylindrical Tubes", Thesis, Stanford University, 1955.

7. Schlicting, H., Boundary Layer Theory, McGraw-Hill Book Co. Inc., 1955, pp. 159-161 and pp. 483-501.

8. Zucrow, M. J., "Discharge Characteristics of Submerged Jets", Bulletin No. 31, Purdue Engineering Experiment Station, 1928.

9. Chen, Chia-Tsun, "Unestablished Flow Patterns Downstream from Square-Edged Pipe Entrances", Thesis, Stanford University, 1952.

10. Reethof, G., Goth, C., and Kord, H., "Thermal Effects in the Flow of Fluids between Two Parallel Flat Plates in Relative Motion", American Society of Lubrication Engineers, preprint number 58 AM 4A-1.

APPENDIX A

SAMPLE CALCULATIONS

properties of petroleum base aircraft hydraulic oil

-5606A (10).

$$\gamma = \gamma_{70^oF} (1 + \lambda\Delta T)$$

$$\lambda = 4.26 \times 10^{-4} \frac{1}{^oF}$$

$$\gamma_{70^oF} = 0.0312 \frac{lb}{in^3}$$

$$\mu = \mu_{70^oF} \quad e^{-\beta\Delta T}$$

$$\beta = 0.01036 \frac{1}{^oF}$$

$$\mu_{70^oF} = 26 \times 10^{-7} \frac{lb\text{-}sec}{in^2}$$

late:

$$\gamma_{150^oF} = 0.0312 \ 1 + 4.26 \times 10^{-4}(80)$$

$$= 0.0323 \frac{lb}{in^3}$$

$$\mu_{150^oF} = 26 \times 10^{-7} \ e^{-0.01036(80)}$$

$$= 11.35 \times 10^{-7} \frac{lb\text{-}sec}{in^2}$$

:e equation:

$$Q = CA \sqrt{\frac{2\Delta P}{\rho}}$$

lculate C, given Q, D, ΔP and γ, the following form of the

ion would be more convenient:

$$C = \frac{Q}{\frac{\pi}{4} D^2} \sqrt{\frac{\gamma}{2(\Delta P)g}}$$

jhout these tests:

$$\gamma = 0.0323 \frac{lb}{in^3}$$

$$g = 386 \frac{in}{sec^2}$$

For the steel test block:

$$D = 0.122 \text{ inches}$$

Substituting these values:

$$C = \frac{Q \frac{231}{60}}{\sqrt{\Delta P}} \quad \frac{1}{\frac{\pi}{4}\,(0.122)^2} \sqrt{\frac{0.0323}{2(386)}}$$

$$= 2.13 \frac{Q}{\sqrt{\Delta P}}$$

From experimental results:

for $Q = 6$ gpm, $\Delta P = 267$ psi

Substituting:

$$C = 2.13 \frac{6}{\sqrt{267}} = .782$$

The abscissa of the experimental plot is easily calculated:

$$\frac{\rho Q}{\mu D} = \frac{Q\,\gamma}{g\mu D} = \frac{6\,\frac{231}{60}\;0.0323}{(386)(11.35 \times 10^{-7})(0.122)} = 139.5 \times 10^2$$

APPENDIX B

DATA

Series A - Plastic Test Block

$D = 0.126$ inch

$e = 5 \pm 1 \times 10^{-6}$ inch rms

$T_s = 150 \pm 5°F$

$L/D = 7.86$ @ $L = 0.990$ inch

Q (gpm)	$P_s - P_e$ (psi)	C	$\frac{\rho Q}{\mu D}$
1	10	.631	22.5 x 100
2	28	.755	44.9 x 100
4	90	.842	90.0 x 100
6	180	.893	135. x 100
8	304	.918	179.5 x 100
10	418	.980	225. x 100
12	551	1.020	250. x 100

Series B - Steel Test Block

$D = 0.122$ inch

$e = 52 \pm 2 \times 10^{-6}$ inch rms

$T_s = 150 \pm 5°F$

$L/D = 8.12$ @ $L = 0.991$ inch

Q (gpm)	$P_s - P_e$ (psi)	C	$\frac{\rho Q}{\mu D}$
1	10	.672	23.25 x 100
2	35	.720	46.7 x 100
4	133	.738	93.5 x 100
6	267	.782	139.5 x 100
8	456	.798	186. x 100
10	619	.855	232.5 x 100
12	833	.887	279.0 x 100
14	1150	.880	326. x 100

L/D = 4.02 @ L = 0.490 inch

Q (gpm)	$P_s - P_e$ (psi)	C	$\frac{\rho Q}{\mu D}$
1	10	.672	23.25 x 100
2	35	.720	46.7 x 100
4	130	.738	93.5 x 100
6	263	.782	139.5 x 100
8	475	.782	186. x 100
10	626	.850	232.5 x 100
12	867	.868	279. x 100
14	1149	.880	326. x 100

L/D = 1.00 @ L = 0.1225 inch

Q (gpm)	$P_s - P_e$ (psi)	C	$\frac{\rho Q}{\mu D}$
1	10	.672	23.25 x 100
2	33	.720	46.7 x 100
4	117	.790	93.5 x 100
6	245	.818	139.5 x 100
8	422	.830	186. x 100
10	594	.875	232.5 x 100
12	816	.887	279. x 100

APPENDIX C

FLOWMETER CALIBRATION

ibration curve for a turbine type flow pickup is a plot of low rate versus the flow pickup output reading in pulses econd. The pulse rate of the flow pickup is measured by ectronic counter. The flow rate through the flow pickup mputed from data for each pulse rate. The time required llect a given weight of fluid is measured. Given the t of fluid flowing per unit time and the weight density e fluid, the volume flow rate may be computed.

r Flowmeter

atory number - 2011

ight oil

rature: 150°F ± 5°F

fic gravity = 0.840

t density (water) = 8.345 lb/gal

$$\gamma_{oil} = \gamma_{water} \times \text{specific gravity}_{oil}$$

$$= 8.345 \times 0.840$$

$$= 7.0 \frac{\text{lb oil}}{\text{gal}}$$

) cycles/sec:

$$1 \text{ gpm} = 400 \frac{\text{cycles}}{\text{sec}} \times 60 \frac{\text{sec}}{\text{min}} \times \frac{50 \text{ lb oil}}{7 \frac{\text{lb oil}}{\text{gal}}}$$

$$= 171{,}500$$

Data

400 Cycle Count	Pulses/Sec	gpm
88625	25	1.94
46045	50	3.73
31313	75	5.48
23503	100	7.30
18641	125	9.20
15602	150	11.00
13499	175	12.7
11800	200	14.5
10482	225	16.4
9388	250	18.4
8543	275	20.1
7808	300	21.9
7206	325	23.8
6685	350	25.8

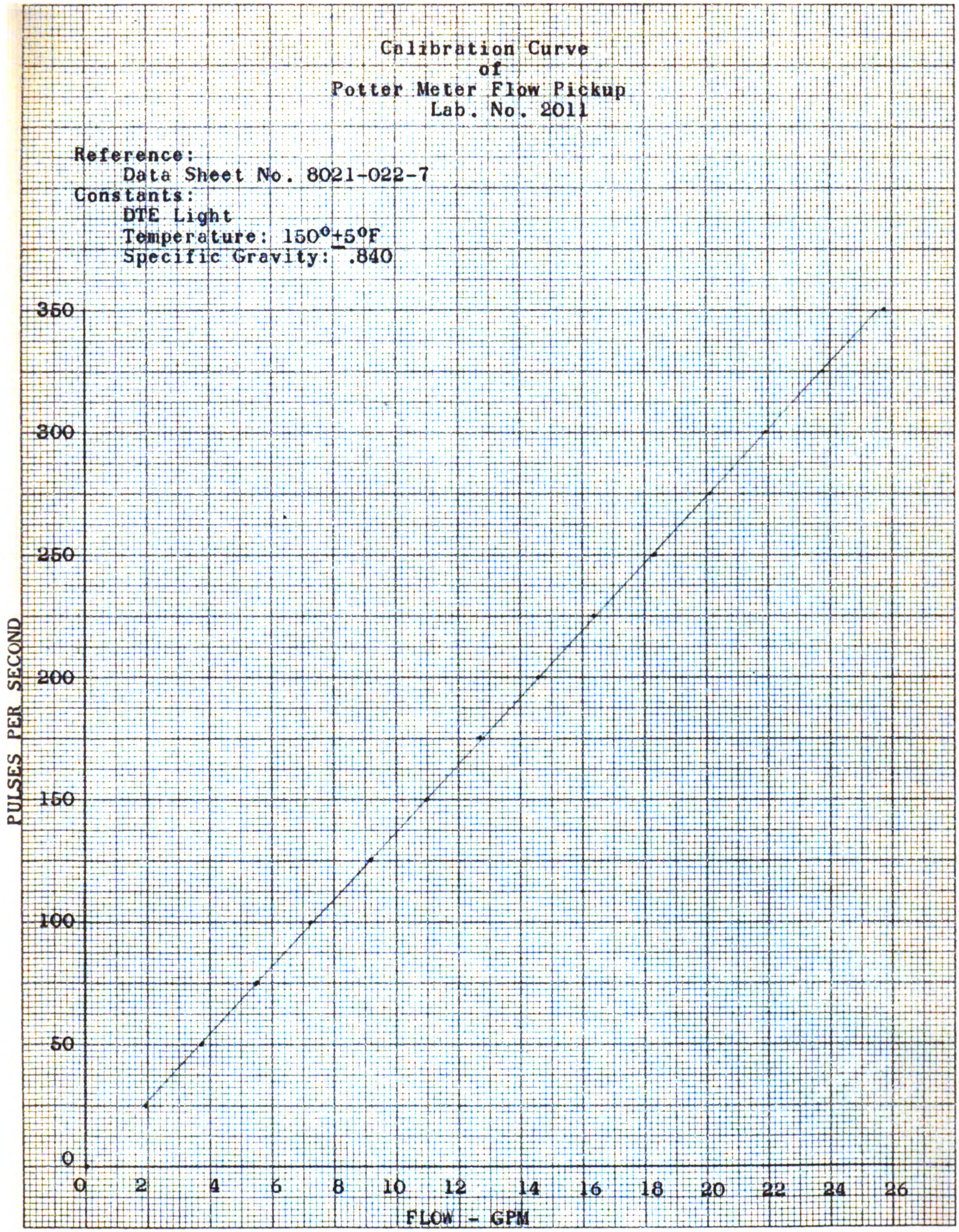
Calibration Curve
of
Potter Meter Flow Pickup
Lab. No. 2011
Reference:
Data Sheet No. 8021-022-7
Constants:
DTE Light
Temperature: 150°±5°F
Specific Gravity: .840
PULSES PER SECOND
0
50
100
150
200
250
300
350
0
2
4
6
8
10
12
14
16
18
20
22
24
26
FLOW - GPM

Figure 12

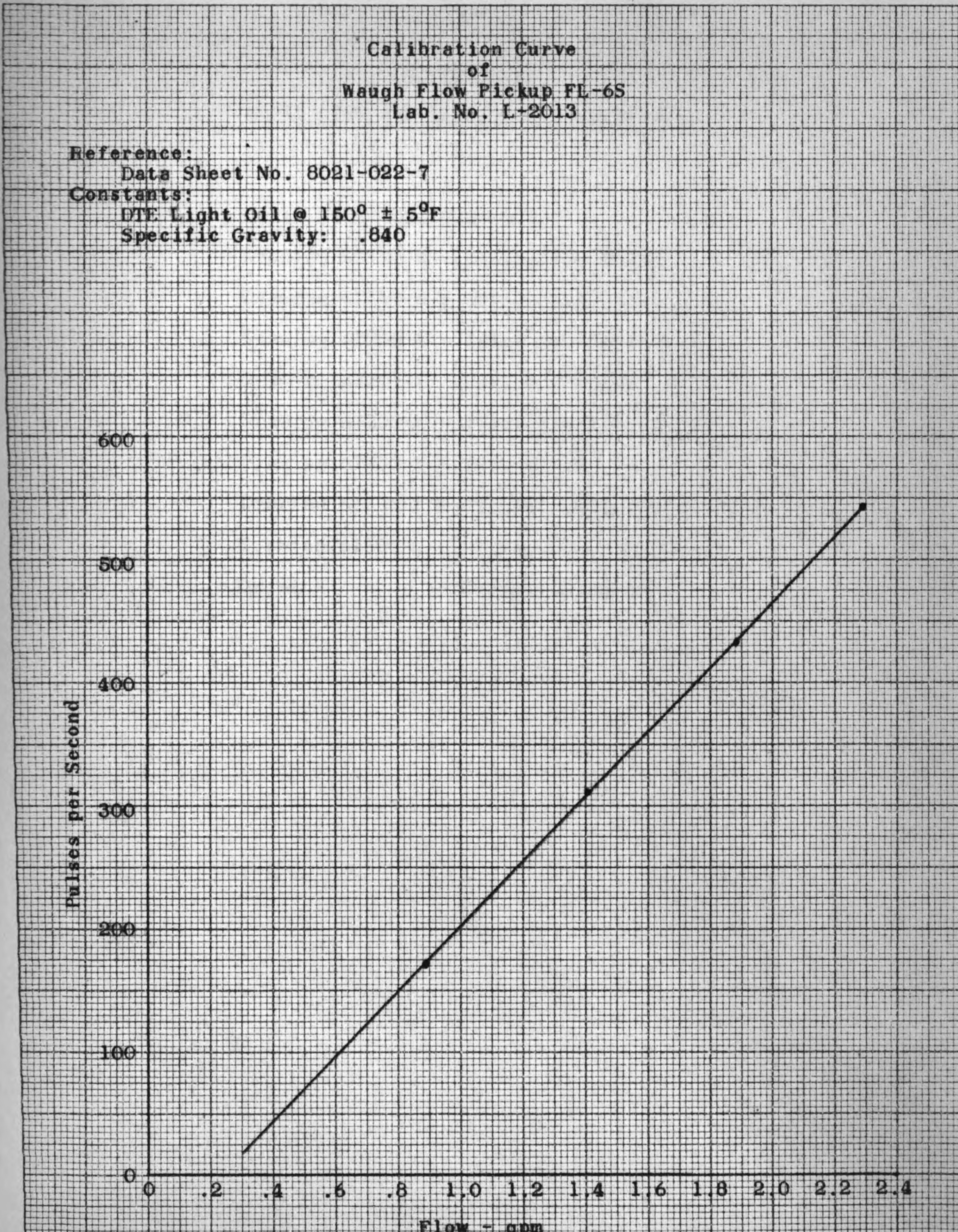
Calibration Curve
of
Waugh Flow Pickup FL-6S
Lab. No. L-2013
Reference:
Data Sheet No. 8021-022-7
Constants:
DTE Light Oil @ 150° ± 5°F
Specific Gravity: .840
Pulses per Second
0
100
200
300
400
500
600
0
.2
.4
.6
.8
1.0
1.2
1.4
1.6
1.8
2.0
2.2
2.4
Flow - gpm

Figure 13

APPENDIX D

PARTS LIST AND DRAWINGS OF APPARATUS

Parts List 8021-022-0101

Drawing 67198-X - Microscope Mount

Drawing 67199-X - Outlet End Plate

Drawing 67200-X - Inlet End Plate

Drawing 67201-X - Outlet Bracket

Drawing 67202-X - Inlet Bracket

Drawing 67203-X - Test Block

Drawing 67204-X - Microscope Mount Slide

Drawing 67205-X - Orifice Test Fixture

Drawing - Circuit Diagram

30

VICKERS INC. DATE 10-17-58 PARTS LIST 8021-022-0101

NAME ORIFICE TEST FIXTURE SHEET NO. 1 OF 1 SHEETS

E. O. 8021-022-1

W. O. NO.

LINE	SIZE	PART NUMBER	NAME	NO. REQ'D
1				
2				
3				
4				
5				
6				
7				
8				
9	E	67205-X	ASSEMBLY	1
10				
11			AND THE FOLLOWING SPECIAL PARTS:	
12				
13	C	67198-X	MICROSCOPE MOUNT	1
14	C	67199-X	END PLATE - OUTLET	1
15	C	67200-X	END PLATE - INLET	1
16	C	67201-X	BRACKET - OUTLET	1
17	C	67202-X	BRACKET - INLET	1
18	C	67203-X	TEST BLOCK	3
19	C	67204-X	SLIDE - MICROSCOPE MOUNT	2
20				
21				
22				
23				
24				
25				
26			AND THE FOLLOWING STANDARD PARTS:	
27				
28		154022	"O"-RING - 70 DUROMETER - 1 1/4 I.D.	2
29		1077-A	3/8 - 16 NC-3 ALLEN CAPSCREW	4
30				
31		8077	#10-24 NC-3 CAPSCREW - 3/4" LONG	8
32		10357	#10-24- NC-3 CAPSCREW - 1" LONG	1
33		8076	#10-24 - NC-3 CAPSCREW - 1/2" LONG	1
34		9706	#10-24-NC-3 CAPSCREW - 5/8"LONG	1
35				
36				
37		1489	1/2-20 NF-3 LIGHT JAM NUT	2
38				
39				
40				
41				
42				
43				
44				
45				
46				
47				
48				

DATE

POSTED

CHANGES

LINE	WAS	DATE	LINE	WAS	DATE	LINE	WAS	DATE
9	REL. FOR T.O.							

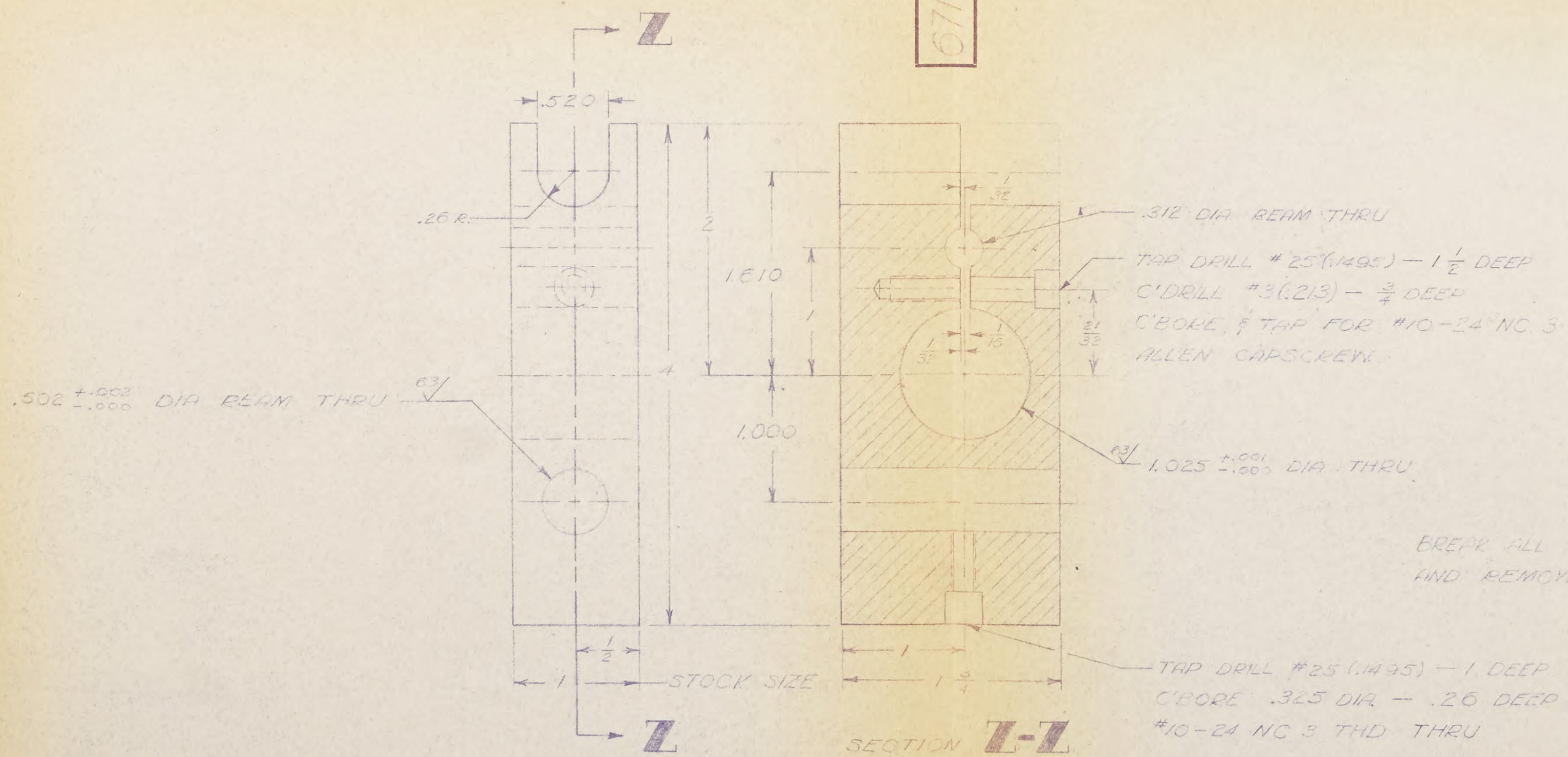

BREAK ALL SHARP EDGES AND REMOVE ALL BURRS.

APPLICABLE SPECS.
MICROFILMED

MACH. PER V. SPEC. MT-

REVISION	DATE	REVISION	DATE
B			

UNLESS OTHERWISE SPECIFIED THE FOLLOWING NOTES APPLY:

MACHINED SURFACE FINISH . 125 √

MACHINED SURFACES INTERSECTING AT RIGHT ANGLES TO BE SQ. WITHIN — PER INCH

ECCENTRICITY TOLERANCES TO BE WITHIN DEC. — FRAC. — T. I. R. —

TOLERANCE ON MACH. DIMS. DEC. ± .005 FRAC. ± 1/64 ANG. ± —

TOLERANCE ON CAST. DIMS. —

MODEL 8021-022-0101	
REF.	
DR. L. SMITH	DATE 10-15-58
CHK. MOLRYK	DATE 10-16-58
PROD. ENG.	DATE
T. O. REL. WAZ	DATE 10-17-58
T. O. NO.	
PROTOTYPE REL.	DATE
PROD. REL.	DATE

VICKERS

VICKERS INCORPORATED
DIVISION OF SPERRY RAND CORPORATION
DETROIT, MICHIGAN U. S. A.

HEAT TREATMENT

MATERIAL 17ST OR 24ST ALUM.

SCALE FULL SIZE

TITLE MICROSCOPE MOUNT

C 67198-X

FORM EN 201 REV. 10-56 1000 9-57 DETROIT BLUE PRINT & SUPPLY CO.

67199-X

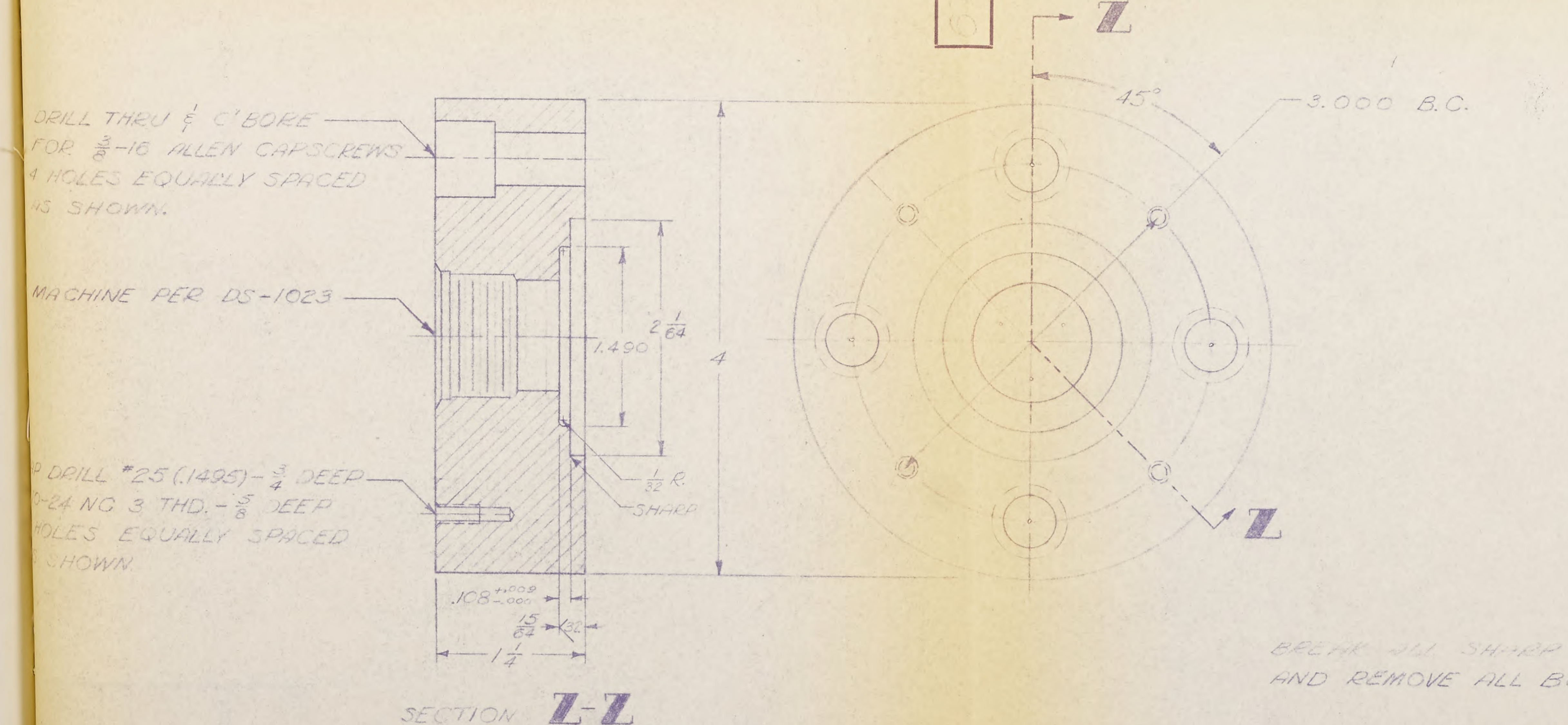

BREAK ALL SHARP EDGES AND REMOVE ALL BURRS.

APPLICABLE SPECS.

MICROFILMED

MACH. PER V. SPEC. MT-

UNLESS OTHERWISE SPECIFIED THE FOLLOWING NOTES APPLY:

MACHINED SURFACE FINISH 125√

MACHINED SURFACES INTERSECTING AT RIGHT ANGLES TO BE SQ. WITHIN — PER INCH

ECCENTRICITY TOLERANCES TO BE WITHIN DEC. — FRAC. — T. I. R. .005

TOLERANCE ON MACH. DIMS. DEC. ± .005 FRAC. ± 1/64 ANG. ± .25

TOLERANCE ON CAST. DIMS. —

MODEL 8081-023-0101

REF.

DR. L. SMITH DATE 10-2-58

CHK. MUDRYK DATE 10-16-58

PROD. ENG. DATE

T. O. REL. [illegible] DATE 10-17-58

T. O. NO.

PROTOTYPE REL. DATE

PROD. REL. DATE

VICKERS

VICKERS INCORPORATED
DIVISION OF SPERRY RAND CORPORATION
DETROIT, MICHIGAN U. S. A.

HEAT TREATMENT

MATERIAL 17ST OR 24ST ALUM.

SCALE FULL SIZE

REVISION	DATE	REVISION	DATE
B			

TITLE END PLATE - OUTLET

C 67199-X

FORM EN 201 REV. 10-56 1000 9-57 DETROIT BLUE PRINT & SUPPLY CO.

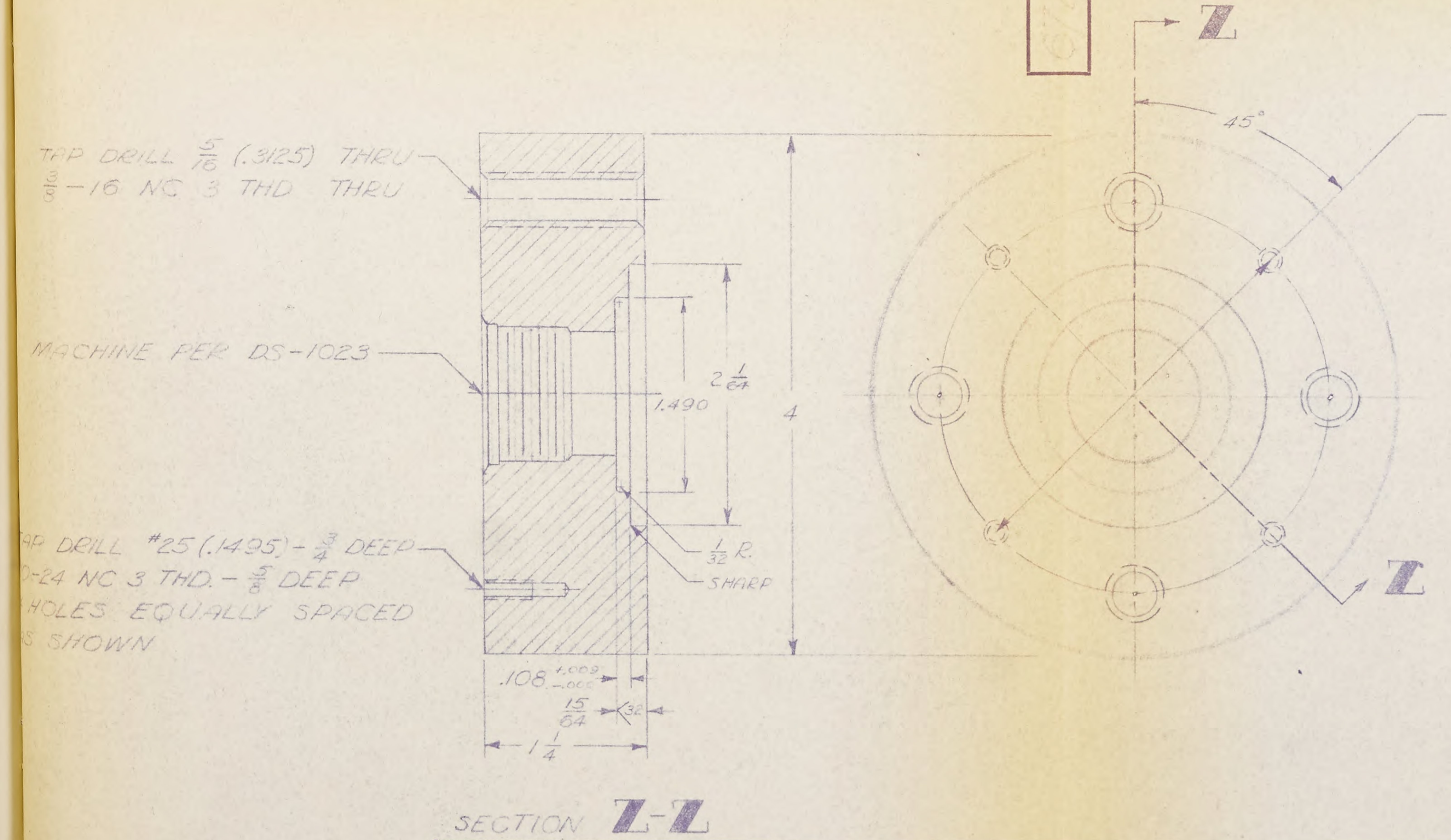

BREAK ALL SHARP EDGES AND REMOVE ALL BURRS.

APPLICABLE SPECS.

MICROFILMED

MACH. PER V. SPEC. MT-

UNLESS OTHERWISE SPECIFIED THE FOLLOWING NOTES APPLY:

MACHINED SURFACE FINISH 125 √

MACHINED SURFACES INTERSECTING AT RIGHT ANGLES TO BE SQ. WITHIN — PER INCH

ECCENTRICITY TOLERANCES TO BE WITHIN DEC. — FRAC. — T. I. R. .005

TOLERANCE ON MACH. DIMS. DEC. ± .005 FRAC. ± 1/64 ANG. ± 2°

TOLERANCE ON CAST. DIMS. —

MODEL	5021-022-0101		
REF.			
DR. L. SMITH		DATE	10-?-58
CHK. MUDRYK		DATE	10-16-58
PROD. ENG.		DATE	
T. O. REL. WJZ		DATE	10-17-58
T. O. NO.			
PROTOTYPE REL.		DATE	
PROD. REL.		DATE	

VICKERS
VICKERS INCORPORATED
DIVISION OF SPERRY RAND CORPORATION
DETROIT, MICHIGAN U. S. A.

HEAT TREATMENT

MATERIAL 17ST OR 24ST ALUM.

SCALE FULL SIZE

REVISION	DATE	REVISION	DATE

TITLE END PLATE - INLET

C 67200-X

FORM EN 201 REV. 10-56 1000 9-57 DETROIT BLUE PRINT & SUPPLY CO.

67201-X

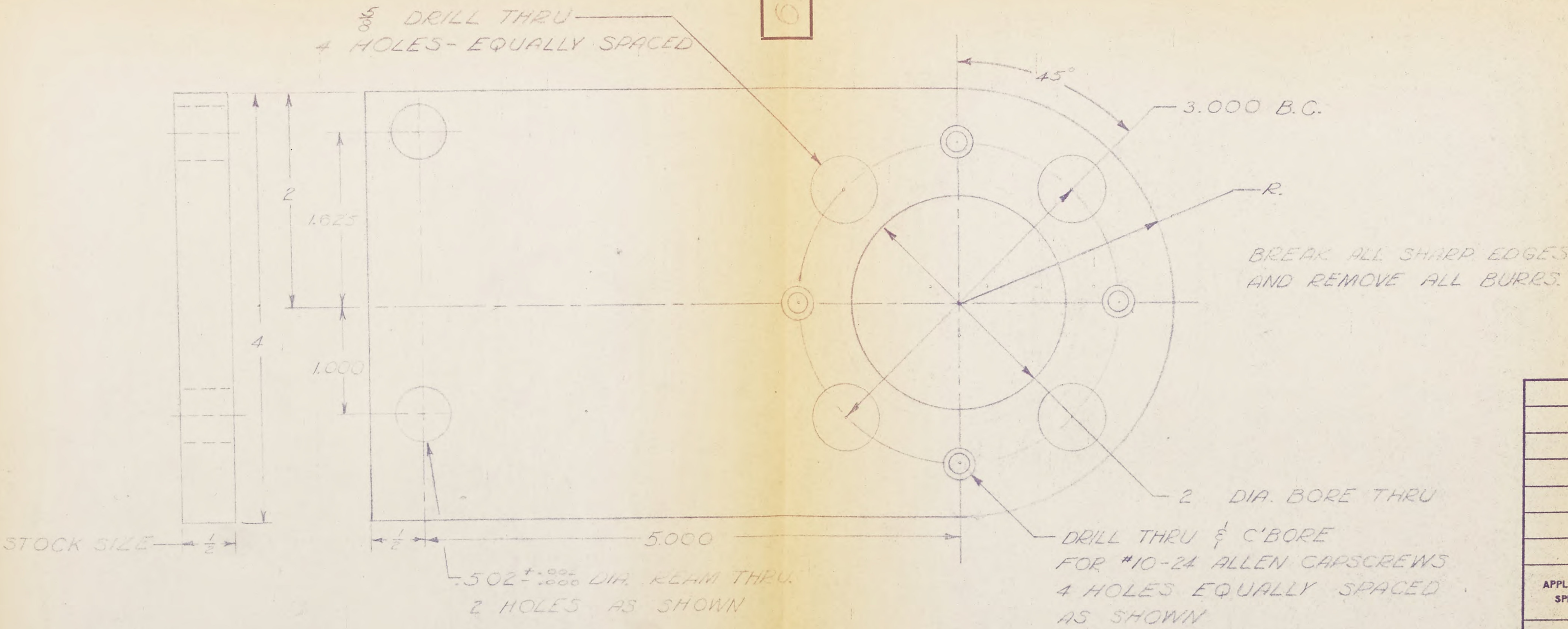

APPLICABLE SPECS.

MICROFILMED

MACH. PER V. SPEC. MT-

REVISION	DATE	REVISION	DATE
93			

UNLESS OTHERWISE SPECIFIED THE FOLLOWING NOTES APPLY:

MACHINED SURFACE FINISH 125√

MACHINED SURFACES INTERSECTING AT RIGHT ANGLES TO BE SQ. WITHIN — PER INCH

ECCENTRICITY TOLERANCES TO BE WITHIN DEC. FRAC. T. I. R. —

TOLERANCE ON MACH. DIMS. DEC. ± .005 FRAC. ± 1/64 ANG. ± 2°

TOLERANCE ON CAST. DIMS. —

MODEL 6021-022-0101	
REF.	
DR. L. SMITH	DATE 10-7-58
CHK. MUDRYK	DATE 10-16-58
PROD. ENG.	DATE
T. O. REL. [illegible]	DATE 10-17-58
T. O. NO.	
PROTOTYPE REL.	DATE
PROD. REL.	DATE

VICKERS
VICKERS INCORPORATED
DIVISION OF SPERRY RAND CORPORATION
DETROIT, MICHIGAN U. S. A.

HEAT TREATMENT

MATERIAL 17 ST OR 24ST ALUM.

SCALE FULL SIZE

TITLE BRACKET - OUTLET

C 67201-X

67202-X

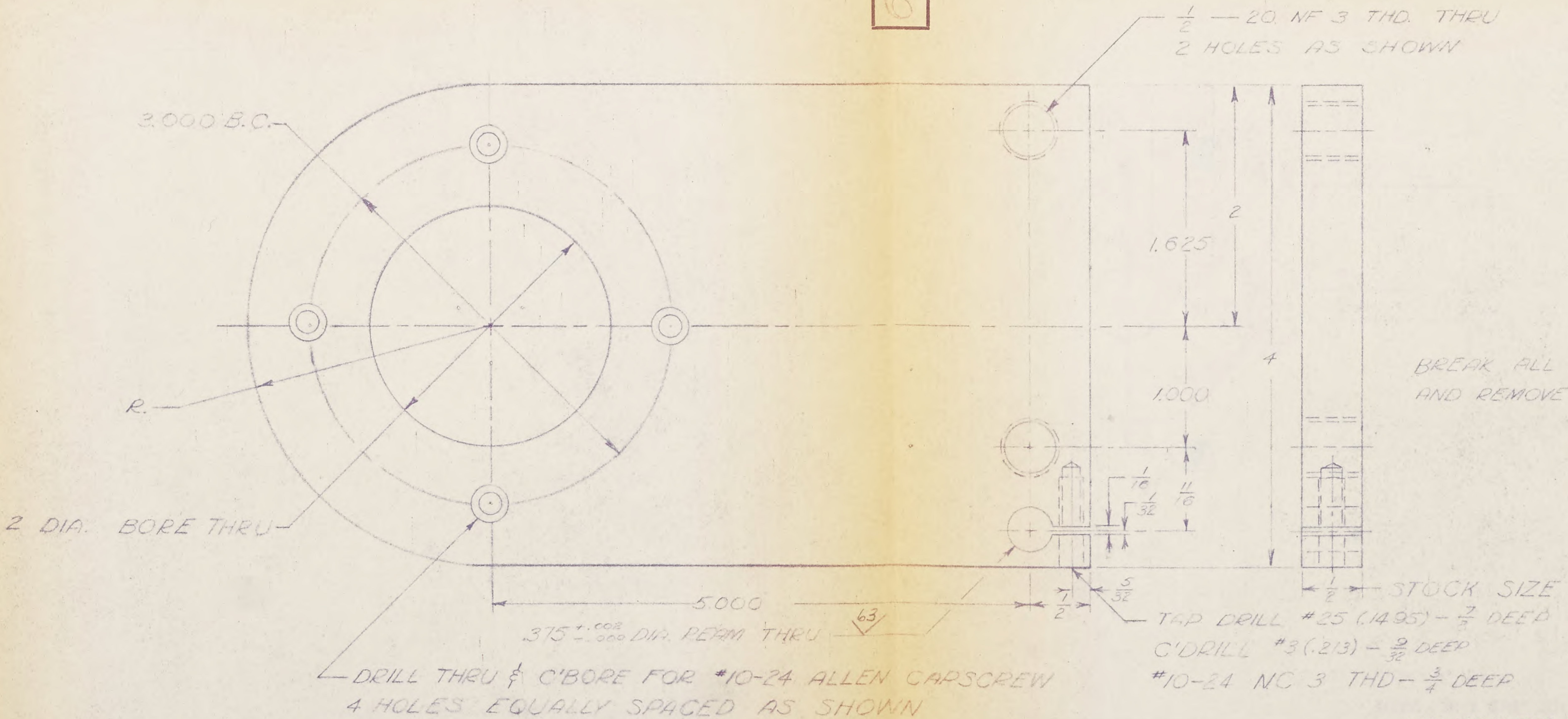

BREAK ALL SHARP EDGES
AND REMOVE ALL BURRS.

APPLICABLE SPECS.

MICROFILMED

MACH. PER V. SPEC. MT-

REVISION	DATE	REVISION	DATE
REVISION VB	DATE	REVISION	DATE

UNLESS OTHERWISE SPECIFIED
THE FOLLOWING NOTES APPLY:

MACHINED SURFACE FINISH 125√

MACHINED SURFACES INTERSECTING AT RIGHT ANGLES TO BE SQ. WITHIN — PER INCH

ECCENTRICITY TOLERANCES TO BE WITHIN
DEC. FRAC. T. I. R. —

TOLERANCE ON MACH. DIMS.
DEC. ± .005 FRAC. ± 1/64 ANG. ± 2°

TOLERANCE ON CAST. DIMS. —

MODEL 8021-022-0101	
REF.	
DR. L. SMITH	DATE 10-7-58
CHK. MODRYK	DATE 10-16-58
PROD. ENG.	DATE
T. O. REL. WJ	DATE 10-17-58
T. O. NO.	
PROTOTYPE REL.	DATE
PROD. REL.	DATE

VICKERS
VICKERS INCORPORATED
DIVISION OF SPERRY RAND CORPORATION
DETROIT, MICHIGAN U. S. A.

HEAT TREATMENT

MATERIAL 17ST OR 24ST ALUM.

SCALE FULL SIZE

TITLE BRACKET - INLET

C 67202-X

67203-X

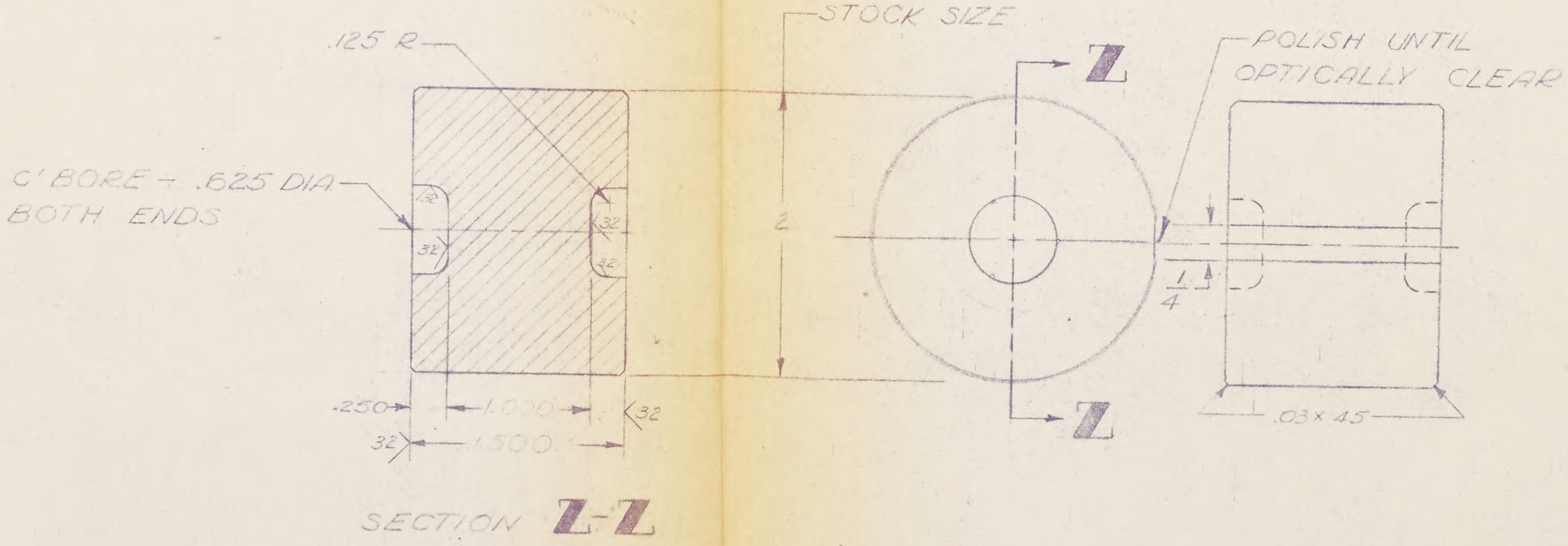

BREAK ALL SHARP EDGES
AND REMOVE ALL BURRS.

MACH. PER V. SPEC. MT-

APPLICABLE SPECS.

MICROFILMED

REVISION	DATE	REVISION	DATE
93			

UNLESS OTHERWISE SPECIFIED THE FOLLOWING NOTES APPLY:

MACHINED SURFACE FINISH 125√

MACHINED SURFACES INTERSECTING AT RIGHT ANGLES TO BE SQ. WITHIN — PER INCH

ECCENTRICITY TOLERANCES TO BE WITHIN DEC. — FRAC. — T. I. R. —

TOLERANCE ON MACH. DIMS. DEC. ± .005 FRAC. ± 1/64 ANG. ± —

TOLERANCE ON CAST. DIMS. —

MODEL	8021-022-0101		
REF.			
DR. SMITH		DATE	10-?-58
CHK. MCDRYK		DATE	10-16-58
PROD. ENG.		DATE	
T. O. REL. WJZ		DATE	10-17-58
T. O. NO.			
PROTOTYPE REL.		DATE	
PROD. REL.		DATE	

VICKERS

VICKERS INCORPORATED
DIVISION OF SPERRY RAND CORPORATION
DETROIT, MICHIGAN U. S. A.

HEAT TREATMENT

MATERIAL LUCITE

SCALE FULL SIZE

TITLE TEST BLOCK

C 67203-X

FORM EN 201 REV. 10-56 1000 9-57 DETROIT BLUE PRINT & SUPPLY CO.

67204-X

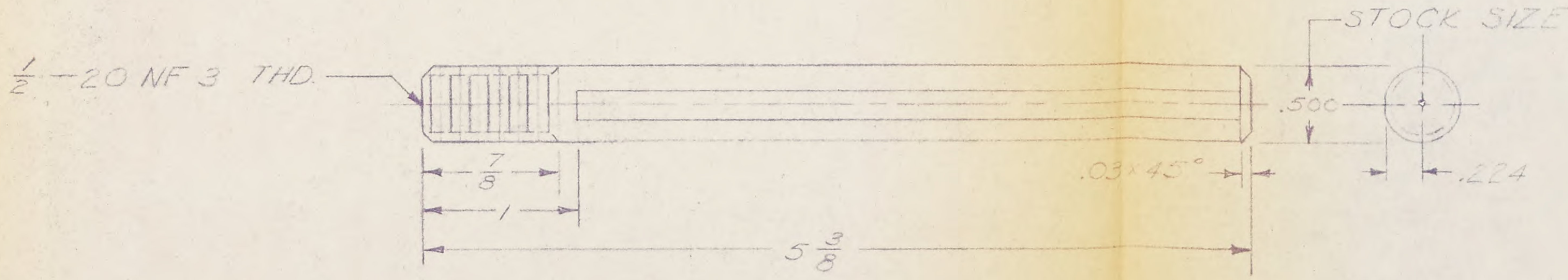

BREAK ALL SHARP EDGES
AND REMOVE ALL BURRS.

APPLICABLE SPECS.
MICROFILMED

MACH. PER V. SPEC. MT-

REVISION	DATE	REVISION	DATE
REVISION 93	DATE	REVISION	DATE

UNLESS OTHERWISE SPECIFIED
THE FOLLOWING NOTES APPLY:

MACHINED SURFACE FINISH 125√

MACHINED SURFACES INTERSECTING AT RIGHT ANGLES TO BE SQ. WITHIN — PER INCH

ECCENTRICITY TOLERANCES TO BE WITHIN
DEC. — FRAC. — T. I. R. —

TOLERANCE ON MACH. DIMS.
DEC. ± .005 FRAC. ± 1/64 ANG. ± 2°

TOLERANCE ON CAST. DIMS. —

MODEL 8021-022-0101	
REF.	
DR. L. SMITH	DATE 10-8-58
CHK. MUDRYK	DATE 10-16-58
PROD. ENG.	DATE
T. O. REL. WJ	DATE 10-17-58
T. O. NO.	
PROTOTYPE REL.	DATE
PROD. REL.	DATE

VICKERS
VICKERS INCORPORATED
DIVISION OF SPERRY RAND CORPORATION
DETROIT, MICHIGAN U. S. A.

HEAT TREATMENT

MATERIAL DRILL ROD

SCALE FULL SIZE

TITLE SLIDE - MICROSCOPE MOUNT

C 67204-X

FORM EN 201 REV. 10-56 1000 9-57 DETROIT BLUE PRINT & SUPPLY CO.

DESCRIPTION

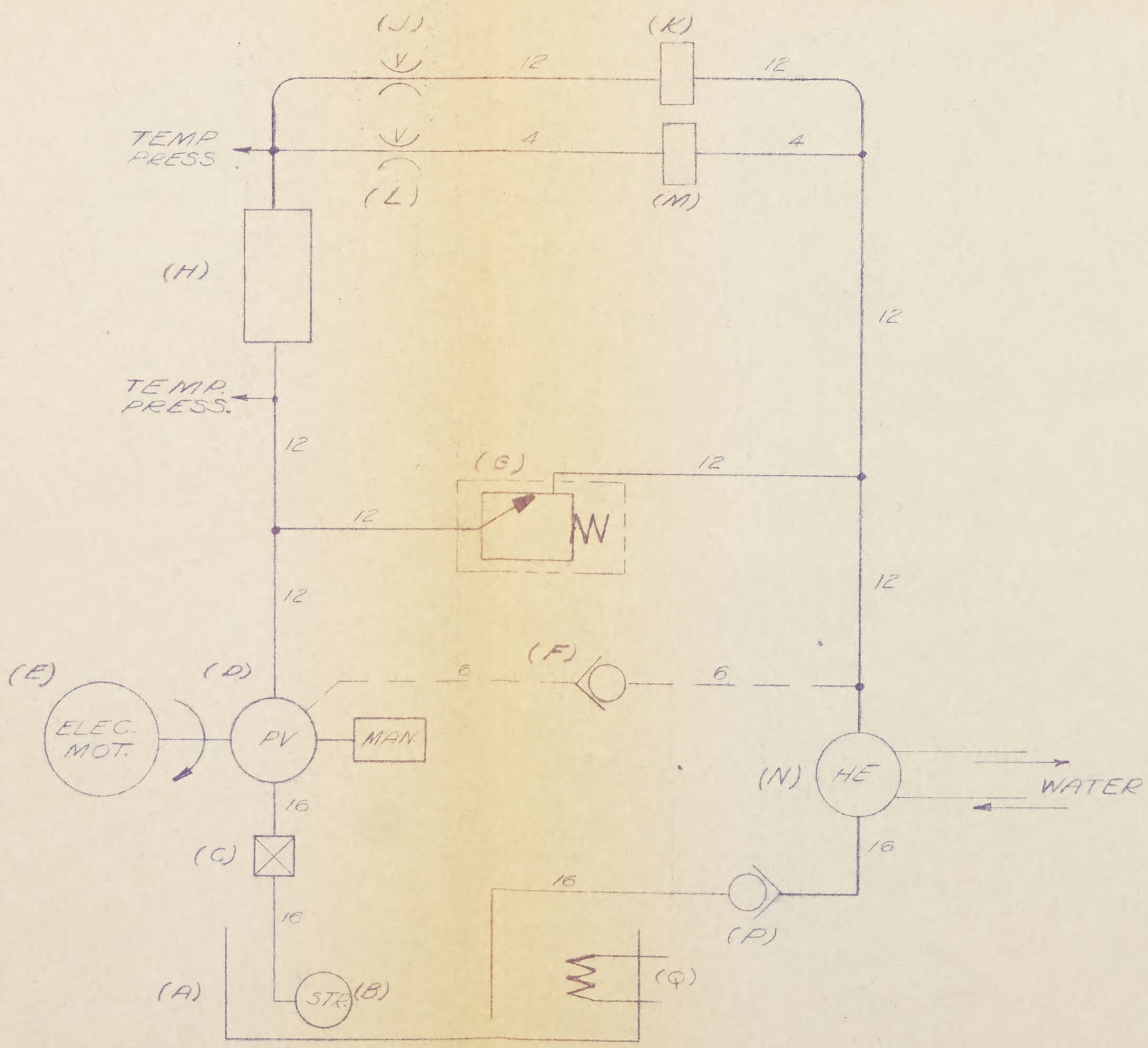

NUMBERS ON LINES INDICATE TUBING SIZE.

KEY	NO. REQ	MODEL NUMBER
A	1	RESERVOIR 10 GALLON
B	1	STRAINER
C	1	1" GATE VALVE
D	1	3913 PUMP VARIABLE
E	1	ELECTRIC MOTOR 25 H.P. 3600 RPM
F	1	3/8" CHECK VALVE
G	1	RELIEF VALVE
H	1	TEST ASSEMBLY
J	1	3/4" NEEDLE VALVE
K	1	3/4" FLOW PICKUP
L	1	1/4" NEEDLE VALVE
M	1	1/4" FLOW PICKUP
N	1	HEAT EXCHANGER
P	1	1" CHECK VALVE
Q	1	HEATER

REVISION DATE

DR. LCS	DATE 12-26-53	FOR VICKERS INCORPORATED	
CHK.	DATE	REL. FOR SALES	REFERENCE
APP.	DATE	TITLE CIRCUIT DIAGRAM R & D TEST GROUP – ORIFICE	

VICKERS INCORPORATED
DETROIT, MICHIGAN

C

EN 328 PRINTED IN U.S.A. 300 1-54 F

D-300